HIGH ENERGY DYNAMIC COMPACTION FOR IMPROVEMENT OF COLLAPSIBLE LOESS

SUMMARY

Prepared by,
Georgios Tsitsas

Directed By:
Professor Dr. Eng. Romeo Ciortan

March 2016

TABLE OF CONTENTS

LIST OF TABLES ..... **ii**

LIST OF FIGURES ..... **iii**

CHAPTER 1: INTRODUCTION **1**

1.1 DYNAMIC COMPACTION AND LOESS 1
1.2 RESEARCH OBJECTIVE 1
1.3 SCOPE OF RESEARCH 2

CHAPTER 2: LITERATURE REVIEW FOR DYNAMIC COMPACTION **2**

CHAPTER 3: LITERATURE REVIEW FOR LOESS **3**

CHAPTER 4: UNDERWATER DYNAMIC COMPACTION **3**

CHAPTER 5: DYNAMIC COMPACTION INDUCED VIBRATIONS **5**

5.1 VIBRATIONS INDUCED BY DYNAMIC COMPACTION 5
5.2 CASE STUDIES 5
5.2.1 Measurements at the Experimental Site 5
5.3 CONCLUSIONS 6

CHAPTER 6: EXPERIMENTAL SITE **13**

6.1 INTRODUCTION 13
6.2 DESCRIPTION OF WORKS PERFORMED 13
6.2.1 Characteristics of the Experimental Site 13
6.2.2 Compaction Tests 14
6.2.2.1 Tests performed during the first phase 14
6.2.2.2 Tests performed during the second phase 14
6.2.3 Compaction grid and energies 14
6.2.4 Enforced settlements 15
6.3 TESTS FOR CERTIFICATION OF THE WORKS 15
6.3.1 General considerations 15
6.3.2 Testing Program 16
6.3.3 Criteria established for improvement certification 16
6.3.4 In situ tests results 16
6.3.5 Laboratory tests results 17
6.3.6 Certification of loess improvement 17
6.4 CONCLUSIONS 18

CHAPTER 7: NUMERICAL ANALYSIS **25**

7.1 INTRODUCTION 25
7.2 BRIEF DESCRIPTION EXPERIMENTAL SITE 25
7.2.1 DC Execution 25
7.2.2 Site Investigation and Soil Properties 25
7.3 METHODOLOGY OF SIMULATION 27
7.3.1 Description of Numerical Methodology 27
7.3.2 Evaluation of Numerical Results 29
7.4 FINDINGS AND DISCUSSION 30
7.5 LIMITATIONS OF CURRENT WORK 31

CHAPTER 8: SUMMARY, CONCLUSIONS AND RECOMMENDATIONS **45**

8.1 INTRODUCTION 45

8.2 RESEARCH OBJECTIVE AND PROJECT SCOPE 45
8.3 EXPERIMENTAL SITE 45
8.4 RESULTS 46
8.5 PERSONAL CONTRIBUTIONS 47
8.6 RECOMMENDATIONS 48
SELECTIVE REFERENCES 49

LIST OF TABLES

Table 5.1: Measurements prior to isolation trench construction 6
Table 5.2: Measurements after isolation trench construction 7
Table 5.3: Measurements after isolation trench construction 7
Table 5.4: Soil particle velocity and possible damages (Rowe 1973) 8
Table 6.1: Energy Parameters 19
Table 6.2: Summary of crater and platform measurements 20
Table 6.3: Parameters obtained from laboratory tests 20
Table 6.4: Direct Shear Tests in compacted soil at different moisture 20
Table 6.5: Ratios of the average values obtained before and after compaction 21
Table 6.6: Values of the tip resistance after compaction 21
Table 7.1: Relationship between φ and N_{SPT} for sands (Peck 1974) 31
Table 7.2: Relationship between φ and N_{SPT} for sands (Meyerhof 1956) 32
Table 7.3: Properties considered in the baseline analysis 32

LIST OF FIGURES

Figure 5.1: Seismograph positions....8
Figure 5.2: Seismograph locations....8
Figure 5.3: Seismograph locations....9
Figure 5.4: Variation of soil particle velocity during DC....9
Figure 5.5: Variation of velocity with magnitude....10
Figure 5.6: Velocity variation with distance....11
Figure 5.7: Velocity variation with number of drops....11
Figure 5.8: Frequency variation with number of drops....12
Figure 6.1: Pounder Tests for first phase of DC....22
Figure 6.2: Pounder Tests for second phase DC....22
Figure 6.3: Average cone tip resistance with depth....23
Figure 6.4: SPT Profile....23
Figure 6.5: Average dry density with depth....23
Figure 6.6: Average porosity with depth....23
Figure 6.7: Average additional settlement index with depth....24
Figure 6.8: Average oedometer modulus at natural moisture with depth....24
Figure 6.9: Average oedometer modulus at saturation with depth....24
Figure 7.1: Experimental Site Location....33
Figure 7.2: Plan dimensions of the steel pounder....34
Figure 7.3: N_{SPT} values before and after DC....34
Figure 7.4: Distribution of stiffness properties with depth before and after DC....35
Figure 7.5: Distribution of friction angle ϕ with depth after DC....36
Figure 7.6: Mesh discretization with the pounder simulated as a rigid steel body....36
Figure 7.7: Applied loading sequence....37
Figure 7.8: Fixed base and quiet boundaries on the left side....37
Figure 7.9: Fixed base and "roller" type boundary conditions at the edge....38
Figure 7.10: Effect of boundary conditions on volumetric strains after 20 drops....39
Figure 7.11: Shear strain contours at different number of drops....40
Figure 7.12: Volumetric strain contours at different number of drops....41
Figure 7.13: Evolution of volumetric and shear strains with depth and number of drops at the center of the pounder....42
Figure 7.14: Effect of soils stiffness and strength on volumetric strains at 14^{th} drop....42
Figure 7.15: Effect of soil stiffness and strength on shear strains at the 14^{th} drop....43
Figure 7.16: Effect of soil properties on the evolution of volumetric strains with depth and number of drops....43
Figure 7.17: Effect of shear strains with depth and number of drops....44

CHAPTER 1: INTRODUCTION

1.1 DYNAMIC COMPACTION AND LOESS

Dynamic Compaction (DC) technique is considered to be one of the oldest forms of ground improvement. It involves repeated dropping of heavy weights (pounders) onto the ground surface and is also known as dynamic consolidation. In the 70's this technique was patented by Louis Menard, in France.

The pounders used for heavy DC may be made of concrete blocks, steel plates, or thick steel shells filled with concrete or sand. In function of their required weight, material and the dynamic bearing capacity at the ground surface, pounders can have square or rectangular in plane section and dimensions. Typically, their mass varies from 10 to 30 tones and they can be left to free fall from heights of 10 to 30 meters (m). For underwater DC, special pounders with wings have been used.

The energy is applied in a controlled pattern of drops using a grid layout. Usually, DC is implemented in two or three phases and for each phase can be applied either single or multiple passes. After each phase the craters are filled with a dozer or filled with granular fill material and then another energy pass is applied. The degree of improvement depends mainly on the energy applied, the mass of the pounder, the free fall height, the grid spacing and the number of drops at each grid point location. Depth of improvement is on the order of 3 to 5 m when lighter pounders and smaller drop heights are used, whereas for heavier pounders and great drop heights it varies from 6 to 12 m.

According to Terzaghi et al. (1936) loess is a uniform, cohesive, wind-blown sediment. It covers about 10% of the earth's surface and can reach thicknesses of 300 m. In Romania, loess and loessial soils deposits cover approximately 17% of the territory or 40,000 km^2. Loess has a metastable structure based on large settlement and loss of strength that may occur upon saturation.

The resistance of the internal structure of loess is given by the cementation occurred between its particles. The cementation bonds are formed mainly by montmorillonite clay and secondarily by calcite. Collapse may occurs due to saturation which leaches out the cementing agents and destroys the bonds of the structure. Local surface saturation can be produced by flooding, broken pipelines, irrigation, or discharge of industrial waters, and may result in significant non-uniform settlements. Regarding a rise of the groundwater table, a slow and uniform increase usually results in uniform gradual settlements. If soil moisture content is increased under an applied load, the resulting settlements may be either gradual settlements or sudden. Also, collapse may occur under critical load, even at a natural moisture content.

1.2 RESEARCH OBJECTIVE

This study was initiated based on the interest of using high energy DC for treating collapsible loess. This report presents site characterization and ground improvement performance results obtained from a 40,000 m^2 experimental site in Constanta, Romania. The scope of the improvement was to treat the ground to depths ranging from 6 to 8 meters in order to reduce settlements and mitigate collapse potential.

To achieve this objective, and based on standard practice with similar projects, are presented the improvement criteria (in situ, laboratory), the special compaction tests and resulting compaction parameters (energy, number of drops, number of phases, etc.) based on actual results from the

experimental site. Other topics of interest were the application of this technique to waterfront projects and vibration monitoring.

Finally, in situ and laboratory results from the experimental site are compared to the results of a finite difference numerical model, developed to simulate the dynamic compaction.

1.3 SCOPE OF RESEARCH

In the last years several motorways are under construction in Romania. The author was involved as chief engineer with three motorway projects where DC was used for improving over 500,000 m^2 of soil, mostly loess.

The first phase of this research took place in 2011 with the execution of the 40,000 m^2 experimental site, in the context of the 22 km Constanta Bypass motorway. The experimental site involved special in situ tests to determine the compaction parameters, and also in situ and laboratory tests for verification of soil improvement. Vibration monitoring was also done at this phase, the results of which are reported herein. These results were evaluated in 2011 and 2012, and related publications were presented between at national and international conferences in 2012-2015 (Iasi, Paris, San Francisco, Edinburgh, and Tirana).

In 2015 DC was numerically simulated with a 2D axi-symmetric model using the Finite Difference Code FLAC. Soil response was simulated using a Mohr – Coulomb elasto-plastic constitutive model. Additional parametric analyses were conducted to evaluate the sensitivity of the results to the assumed material properties and other parameters.

CHAPTER 2: LITERATURE REVIEW FOR DYNAMIC COMPACTION

Chapter 2 provides background on the development of DC, theoretical aspects, and considerations related to design, quality control, etc.

The specific elements of this procedure are the simplicity of the technique used and its extreme complexity from the point of view of both soil mechanics and the obtained safety, which is approved by the obtained results.

Simplicity: nowadays, high capacity lifting machines are used and they can produce intensities of 100 to 500 higher than the ones necessary for driving piles.

Extreme complexity: from the point of view of soil mechanics, DC technique leads to a new spirit in this domain. This technique can develop on an “open field” from which traditional boundaries can be overcome.

Safety: is provided by the experience gained from various consolidation works, geotechnical control of the obtained results and observations on construction settlements;

This new consolidation technique opens a wide market for soil mechanics due to the fact that in-situ measurements are about three times more than in the case of direct foundations on unconsolidated soils (example: piles foundations).

In addition to classic construction domains new perspectives regarding the application of DC technique are targeted: soil dams placed on soils with poor geotechnical characteristics, artificial islands, etc.

Also, this method allows the construction of works without any special treatment for stabilization and soil, the most famous material, becomes structural.

CHAPTER 3: LITERATURE REVIEW FOR LOESS

Chapter 3 is literature review on loess and offers an overview of collapse mechanism, characteristic parameters, and describes research where CPT testing is used to evaluate instability phenomena under cyclic loading.

Collapsible loess is a macro-porous, unsaturated silty soil that is stiff in its natural state. In contact with water it exhibits sudden and irreversible changes of internal structure. The most commonly accepted theory to explain its origins is the aeolian theory. Furthermore, collapse phenomena occur due to saturation that disturbs the natural structure of the soil, destroys the capillarity bonds and the clay bonds, and leaches out the cementing agents. Collapse results in quick and non-uniform settlement which may cause major degradations to the structures built over such soils.

Settlement due to saturation can be determined in the laboratory by conducting oedometer compressibility tests. Based on these tests are determined the additional settlement index ($i_{m\sigma}$), according to Romanian standards or the collapse potential (C_p), according to ASTM. The final value of the settlement is computed by multiplying the additional settlement index, respectively the collapse potential, with the thickness of the collapsible soil layer. Recent research has been done with CPT-V_s correlations for the evaluation of instability issues due to cycling loads.

There are various methods to mitigate risks when constructing over collapsible soils. In terms of ground improvement, there are different options such as mixing with additives, compacting, introducing structural elements and replacement. All these techniques may be used to improve soil over its entire deformable/collapsible zone.

CHAPTER 4:UNDERWATER DYNAMIC COMPACTION

Chapter 4 gives information about DC applications for marine and waterfront jobs, including special equipment, case studies from various countries and local experience, and for both improvement of foundation soil, as well as for consolidation.

Based on local experience and international projects, DC is a technique that can be used to improve foundation soil or to consolidate fill underwater. In addition, from performed measurements and observations the following conclusions can be drawn:

- Due to pounder deviation during the free fall, the drop locations will overlap
- The last phase of DC (the levelling phase) will be executed using 20÷40 mm crushed stone
- The pounder will be submerged during the entire operation

- The pounder will be manufactured such to be stable underwater - this can be accomplished by adding stabilization wings
- The pounder will be manufactured such to obtain the maximum weight on the unit surface
- The water depth should be of minimum 4 m in order to obtain an effective compaction for a layer of maximum 2 m thickness
- For smaller water depths, will be analyzed the possibility of applying DC in “dry conditions”, by filling the area with cohessionless soil that later will be dredged
- The thickness of the compacted layer must be correlated with the free fall height of the pounder which is dependent on water depth

CHAPTER 5: DYNAMIC COMPACTION INDUCED VIBRATIONS

Chapter 5 involves measurements from vibration monitoring from the experimental site and provided comparisons to data published in literature.

5.1 VIBRATIONS INDUCED BY DYNAMIC COMPACTION

Due to the wide range of impact loads that can be applied on soils during DC, a wide range of ground vibrations appear. As the soil is densified, vibration level increases. It is possible to achieve a maximum particle velocity after only one or two passes of heaving tamping.

Elastic waves transmitted in all directions are induced during DC. The soil vibration spectra induced by tamping have a few maximum values with the dominant frequency of the surface wave. Since these frequencies are identical with the natural frequencies of soil layers, their values do not depend on the conditions from the contact area where impacts are directly applied on soils. However, when pounders of different sizes are used, the impacts on the same contact area might generate surface waves with different dominant frequencies. Moreover, the value of the dominant frequency depends mainly on the applied impact as soil is nonlinear (Svinkin et al. 2000).

5.2 CASE STUDIES

Dynamic Compaction technique induces vibrations which are felt on a certain distance from the impact point, affecting in this manner the adjacent buildings. For this purpose, measurements were performed such to determine the working area with this technology.

5.2.1 Measurements at the Experimental Site

Vibration monitoring was used at the experimental site at Valul lui Traian due to the presence of a nearby oil pipe. In order to establish the distance up to which DC technique can be applied such not to damage the oil pipelines crossing the area, the induced vibrations were measured. A maximum velocity of 20 mm/sec of the soil particles was imposed for pipelines.

Experiments were performed in two cases:

- Without taking any measure to isolate the effects induced by DC technique (Figure 5.1 and Table 5.1)
- A 3 m deep trench was constructed between the working area and the pipelines at about 15 m distance from the pipelines (Figure 5.2 and Table 5.2, Figure 5.3 and Table 5.3)

The analysis was performed taking into consideration the possible degree of degradation (Rowe, 1973) that produces for different soil particle velocities (see Table 5.4):

Some authors recommend not to exceed the value of 50 mm/sec for soil particle velocity.

In order to determine the manner in which soil particles velocity varied with distance the results obtained from the experimental site were plotted together with the results of other experiments that were taken into consideration (Figure 5.4).

The acceptable limit for soil particle velocity and type of construction indicated by French Technical Specification is shown in Figure 5.5. Measurements from the experimental site

performed before and after trench construction, were plotted on this graph and it resulted that after the trench was constructed, all recorded velocities are smaller than the admissible value (20 mm/sec).

Based on measurements obtained from the experimental site and on provisions from technical specifications were established the vibration parameters that do not affect the oil pipelines:

- The trench was constructed up to 0.5 m below the bottom of the pipe
- The trench was constructed at 15 m distance from the oil pipelines
- The minimum distance between the axis of the pipe and the compacted area was of 15m
- The allowable velocity for soil particles was of 20 mm/sec

Figure 5.6 shows that the velocity decrease as the distance from the impact point increases.

Graphical representation of both velocity (Figure 5.7) and frequency (Figure 5.8) against number of free falls indicate that both of them increase with each applied blow.

5.3 CONCLUSIONS

Ground acceleration was measured using a seismograph placed at different distances from the compacted area. Based on recorded data the following were found:

- Vibration frequency is influenced by the number of free falls and it is more obvious at smaller distances
- Soil particle velocity increases slower to a total number of four drops; after that it increases faster
- The trench reduced with approximately 20% the velocity of soil particles
- Soil particle velocity decreases with distance

Table 5.1: Measurements prior to isolation trench construction

Number of free falls	Distance with respect to the crater(m)	Velocity (mm/s)	Frequency (Hz)
1	14	20.66	8.3
2		27.6	14
3		37.6	16
4		42.3	17
5	20	25	13
6		24.8	13
7	25	21.5	12
8		22	12
9		20.7	12
10	30	12.8	12
11		14.9	12
12		14.9	13
13	35	6.73	9.1
14		6.6	9

Table 5.2: Measurements after isolation trench construction

Number of free falls	Distance with respect to the crater(m)	Velocity (mm/s)	Frequency (Hz)
1	35	0	0
2		0	0
3		7.37	10
4		9.14	11
5		10.2	13
6		10.4	11
7		10.9	12
8		10.9	11
9		9.4	9.8
10		9.65	12
11		11.9	12
12		12.8	12

Note: at 35 m distance from the crater 863

Table 5.3: Measurements after isolation trench construction

Number of free falls	Distance with respect to the crater(m)	Velocity (mm/s)	Frequency (Hz)
1	28	0	0
2		4.95	12
3		6.48	8.8
4		7.75	19
5		8.76	9.8
6		9.40	20
7		9.52	18
8		9.52	10
9		10.3	10
10		10.7	10
11		11.4	11
12		12.6	11

Note: at 28 m distance from the crater 933

Table 5.4: Soil particle velocity and possible damages (Rowe 1973)

Maximum soil particle velocity (mm/sec)	Building damages
0,2	None
2,0	Superior limit for historical monuments, very fragile structures
5,0	Inferior limit for architectural damages of buildings with sensitive finishing layers
15,0	Architectural damages and possible structural damages
50,0	Structural damages of buildings that do not enter in the resonance domain

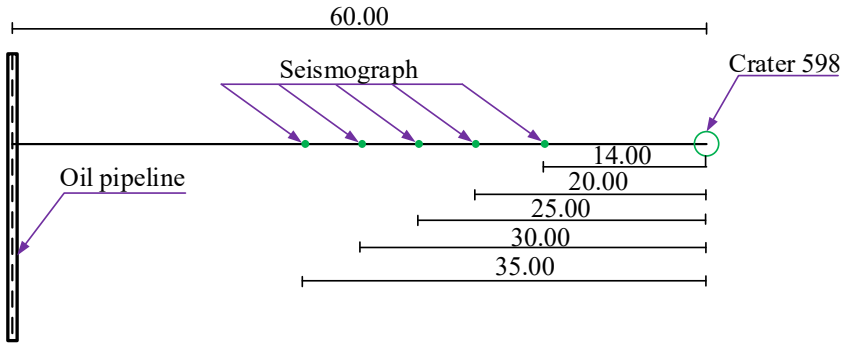

Note: refers to crater 598, without isolation trench

Figure 5.1: Seismograph positions

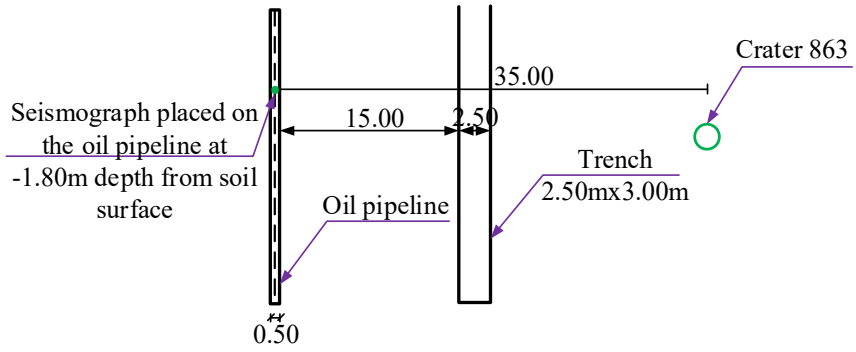

Note: at 35 m distance from the crater 863 – With isolation trench

Figure 5.2: Seismograph locations

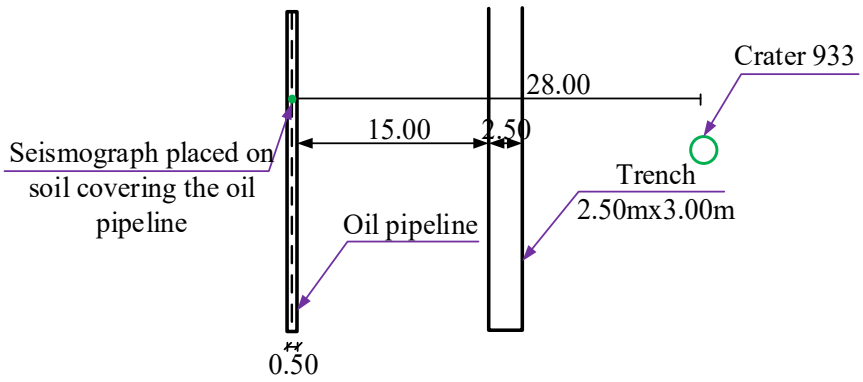

Note: at 28 m distance from crater 933 – With isolation trench

Figure 5.3: Seismograph locations

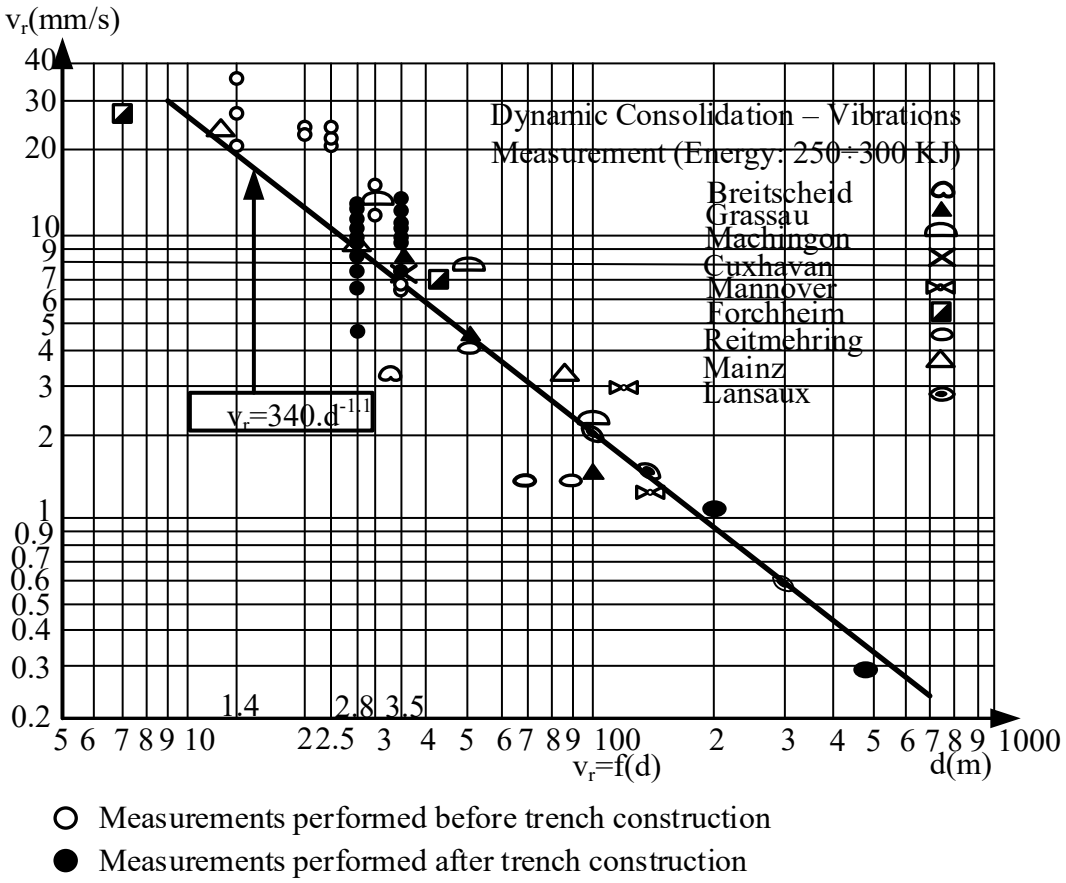

○ Measurements performed before trench construction

● Measurements performed after trench construction

Figure 5.4: Variation of soil particle velocity during DC

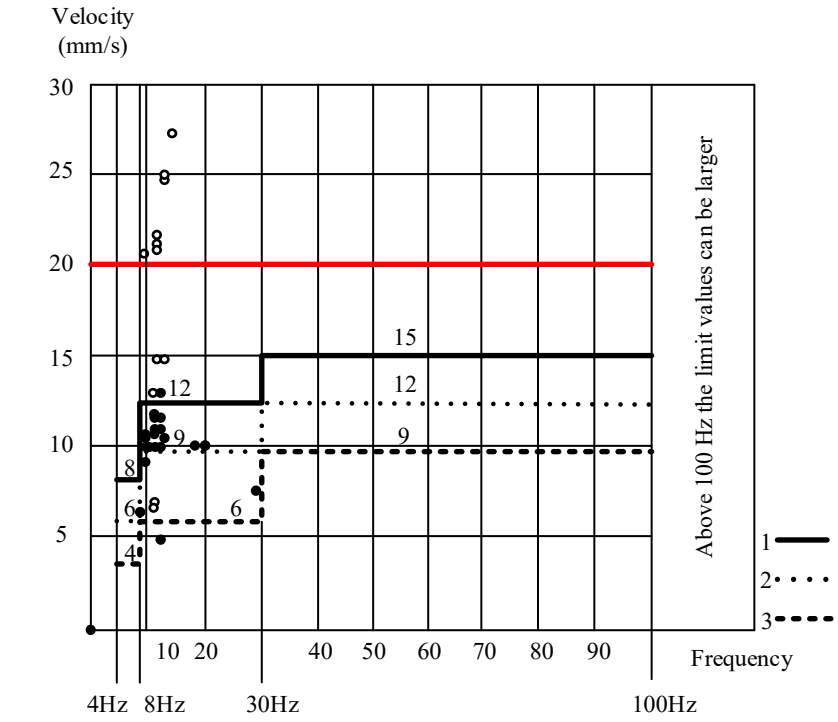

Curves
1 Corresponds to non sensitive structures such as reinforced concrete structures
2 Corresponds to sensitive structures such as masonery, buried sewer pipes, non reinforced concrete structures
3 Corresponds to highly sensitive structures such as fissures buildings, buried gas pipes etc.
4 Corresponds to the admissible velocity (20mm/sec) imposed for the oil pipelines

Measurements performed before trench construction

Measurements performed after trench construction

*Note: Vibration threshold values must be given or confirmed by the owner of the concerned structure

Figure 5.5: Variation of velocity with magnitude

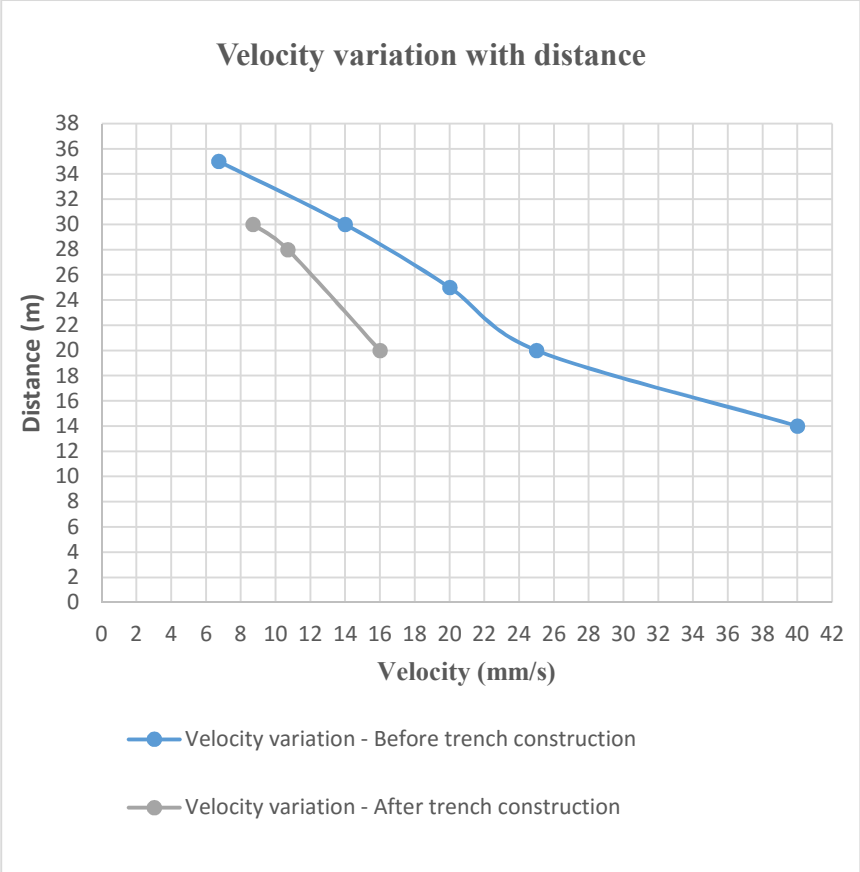

Figure 5.6: Velocity variation with distance

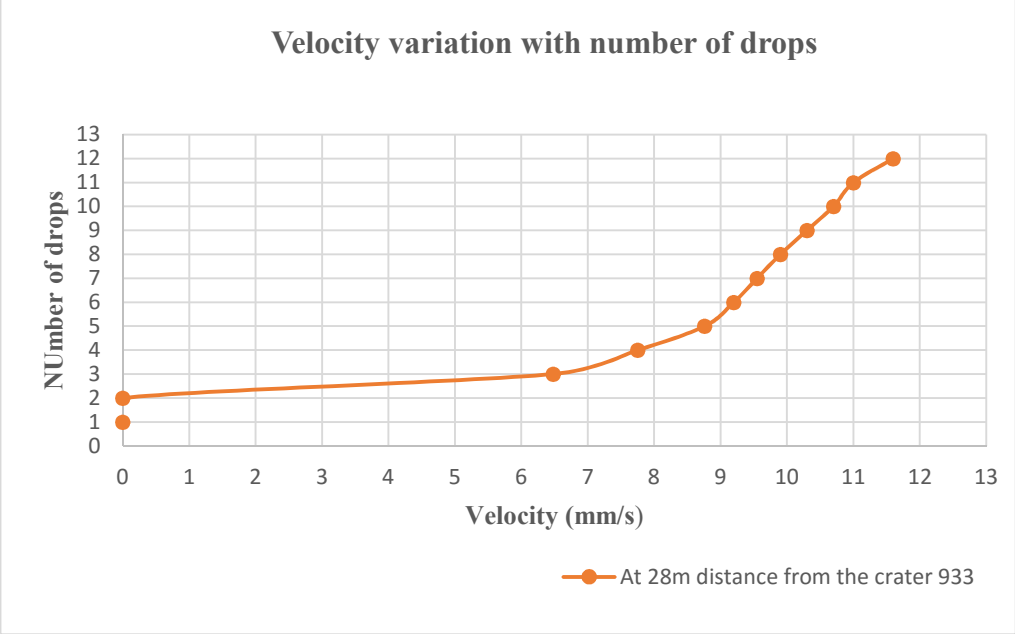

Figure 5.7: Velocity variation with number of drops

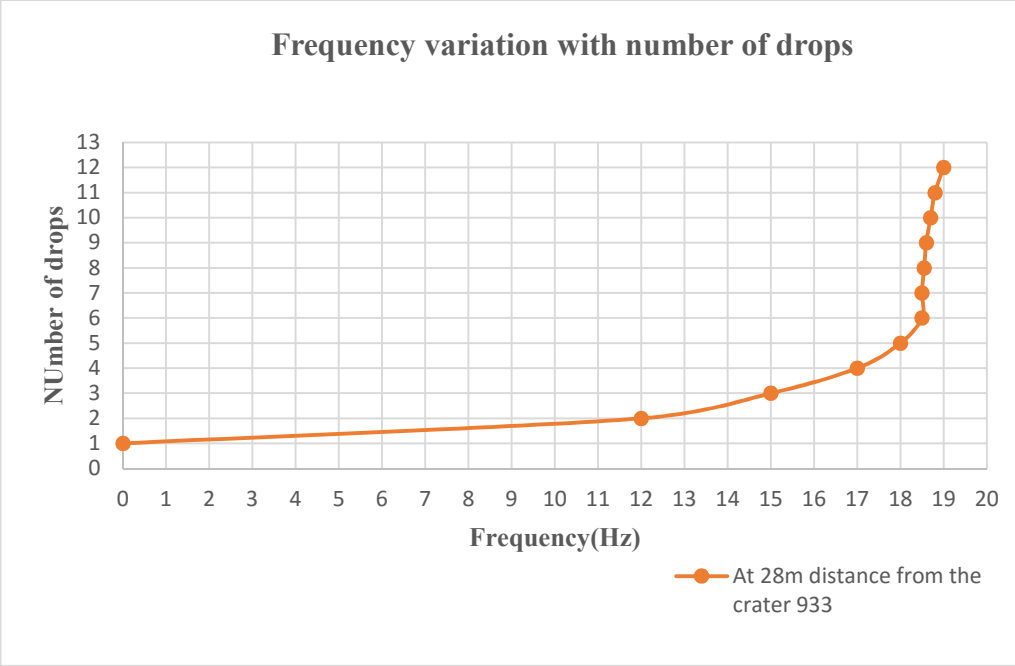

Figure 5.8: Frequency variation with number of drops

CHAPTER 6:EXPERIMENTAL SITE

6.1 INTRODUCTION

The experimental site of approx. 40,000 square meters (m^2) is located in Constanta area and more specifically at Valul lui Traian in the vicinity of the railway line Bucharest – Constanta. On this site was performed high energy Dynamic Compaction (DC) to treat collapsible loess. Various tests have been performed and are presented in this chapter including compaction tests, as well as in situ and laboratory tests. All the work on site presented below has been organized and managed by the author for both its engineering and execution components.

Prior geotechnical investigations revealed the existence of a 12 m thick loess deposit below which is a layer of red clay with limestone concretions. It was determined that the first 6 meters of loess were sensitive to water. Under depths of about 28 m to 40m is bedrock which consists of degraded limestone in clay mass. Groundwater level has been measured to depths below 12 meters.

Then, when considering transportation projects such as motorways, the nature and grade of consolidation of the ground and the necessity to limit differential settlements, dictates the implementation of ground modification. For the purpose of this study the selected method was DC.

For the design, development and verification of the experimental site, have been undertaken specific in situ and laboratory tests, and calculations that led to defining both the technological process of dynamic compaction and the certification procedure for confirming the quality results. In addition, as described in Chapter 7, a finite difference program has been used for additional confirmation. Vibration monitoring results have been included in Chapter 5.

Based on the results obtained by processing this data can be established the compaction parameters for execution and criteria for quality control of the works. The following sections present the methodologies and criteria proposed for certification of loess improvement by DC, as well as the type of compaction tests, the determined compaction parameters and the in situ and laboratory results from the 40,000 m^2 experimental site.

6.2 DESCRIPTION OF WORKS PERFORMED

6.2.1 Characteristics of the Experimental Site

The geometrical features of the experimental site are the following:

- length = 490 m
- maximum width = 83 m
- minimum width = 80 m
- total area = 39,997 m^2
- area compacted = 30,176 m^2

The geology in the area is fairly uniform with:

Layer I	Clayey Silt (loose)	0 to -4 m (collapsible layer)
Layer IA	Silty Clays (soft)	-4 to -8,5 m (compressible layer)
Layer IB	Silty Clay (stiff)	-8,5 to -10 m
Layer II	Bedrock Weathered	below -10 m
Layers III and IV	Bedrock	

Layers II to IV are considered uncompressible.

6.2.2 Compaction Tests

In order to control the soil reaction to dynamic compaction several tests were carried out for both, first phase and second phase. They consisted of pounder penetration tests and heave tests.

6.2.2.1 Tests performed during the first phase

During the first phase of compaction were performed 6 pounder penetration tests at the location of the craters: 74, 119, 185, 360, 791 and 811. The graphs are presented in Figure 6.1.

Except the test performed at crater number 791, which showed an increased penetration depth with 2.8 m for 12 blows and a 12.99 m^3 volume, all pounder penetration tests show a fairly homogeneous reaction with:

	U.M.	12 blows	14 blows
Pounder penetration	**(m)**	**2.19**	**2.34**
Crater average volume	(m^3)	12.44	13.76
Enforced settlement	(cm)	25.4	28.1
Resulting volume reduction	(%)	4.23	4,68

Three heave tests were performed at crater locations number 185, 360 and 791. No heave was measured.

6.2.2.2 Tests performed during the second phase

During the second phase of compaction were performed 6 pounder penetration tests at the location of the craters: 1039, 1071, 1130, 1552, 1581 and 1721. The results are shown in graph from Figure 6.2.

Except the test performed at crater number 1721, which showed an increased penetration depth with 2.56 m for 12 blows and the volume with 12.42 m^3, all pounder penetration tests show a fairly homogeneous reaction with:

	U.M.	12 blows	14 blows
Pounder penetration	(m)	1.79	1.88
Crater volume	(m^3)	9.81	11.26
Enforced settlement	(cm)	20.00	23.00
Volume reduction	(%)	3.34	3.83

Three heave tests were performed at crater locations number 1071, 1552 and 1581. No heave was measured.

6.2.3 Compaction grid and energies

The compaction was conducted in 3 phases as described in Table 6.1. At beginning of each phase was conducted a pounder penetration test in order to optimize the number of blows (see Figure 6.1 and Figure 6.2).

It was established, based on various requirements, that the dynamic compaction technique must enforce a volume reduction at 6.5%.

Therefore, the compaction energy was applied with 12 blows for both phases which assured a volume reduction of 10% including the ironing phase. Nevertheless the number of blows has been modified during execution taking into account the variations of the local soil reaction (12 to 14 blows).

Due to the presence of an oil pipe, dynamic compaction could not be performed within a 20 m buffer zone along the pipe line. Issues related to vibrations have been discussed in Chapter 5.

6.2.4 Enforced settlements

For the first 2 phases the crater dimensions have been measured and the total crater volume have been calculated.

For the 1st, 2nd and ironing phase, a level survey of the compaction zone is performed before and after to measure accurately the lowering of ground level under DC impacts.

The total volume of all craters is divided by the number of craters to derive the average print volume which is then divided by 49 m^2 to calculate the phase mean enforced settlement:

S_{DC} = Vol/Unit Area

Table 6.2 gives the summary of the results.
The enforced settlement related to a compacted thickness of 6 m gives a total strain of:

$\Delta H/H = 12.6\%$

If we consider 8 m of collapsible/compressible soil, the volume reduction becomes:

$\Delta H/H = 9.4\ \%$

The above values are meeting the specification in terms of densification ratio.

6.3 TESTS FOR CERTIFICATION OF THE WORKS

6.3.1 General considerations

As mentioned in Chapter 3, loess is sensitive to saturation; it is a deposit characterized by the tendency to collapse in presence of water, leading to the appearance of “additional settlement” under construction loads (Group A) or even under its own weight (Group B). In most cases “additional settlement” is differential due to uneven distribution of large volume voids, usually over 40%.

The application of dynamic compaction technology to mitigate the risk of additional settlements, which are usually uneven, of loess is based on the mechanism of modifying the state of consolidation by braking the bond formed between the solid particles and rearranging them, decreasing the porosity, and, at the same time, increasing the volume occupied by the mineral skeleton. Thus, global compressibility is reduced.

6.3.2 Testing Program

Taking into account the above considerations and the provisions of related technical norms, to certify the quality of the improvement works by compaction on a depth of approximately 6 m, was proposed and implemented a program of in-situ and laboratory tests before and after compaction.

This program contained:

- in situ tests including SPT and CPT and geotechnical borings with disturbed and undisturbed samples and depths over 6m (8 – 12 m)
- laboratory tests to determine the grain size, densities in various states, porosity, moisture, plasticity and consistency and also double oedometer tests (oedometer modulus $M_{200\text{-}300}$)

To compute the bearing capacity of the compacted ground were executed tests to determinate the direct share resistance parameters, including the angle of internal friction ø and cohesion c. Where made U.U. (Unconsolidated – Undrained) and C.U. (Consolidated – Undrained) direct share tests.

6.3.3 Criteria established for improvement certification

In order to consider that loess is no longer sensitive at saturation the following criteria were established (Manea et al. 2012):

- Decreasing the additional settlement index $i_{m300} < 2\%$
- Increasing the dry density $\rho_d > 1.6$ g/cm^3
- Reduction of the porosity $n < 40\%$
- Increasing the average oedometer modulus $M_{200\text{-}300}$ at natural moisture and saturation
- Increasing the average tip resistance $q_c > 2.5$ MPa

To characterize the ground improvement by DC of the loess up to 6 m depth, are compared the average values of the above mentioned parameters obtained before and after compacting.

Also, in order to certify the quality of the works the following conditions have been established:

- $i_{m300comp} / i_{m300nat} < 1$
- $\rho_{d\ com} / \rho_{d\ nat} > 1$
- $n_{com}/n_{nat} < 1$
- $M_{200\text{-}300\ com} / M_{200\text{-}300\ nat} > 1$
- $M_{200\text{-}300\ com\ sat} / M_{200\text{-}300\ nat\ sat} > 1$

6.3.4 In situ tests results

For in-situ verifications were performed fifteen cone penetration tests (CPT) and two standard penetration tests (SPT) till depths of approximately 8 – 12 m. The results of CPT indicate a significantly increase of q_c from 1 – 1.5 MPa to 2.5 – 3.5 MPa.

The improvement based on average values obtain from CPT can be quantified as following:

- From 0 m to -3 m: improvement 225%
- From -3 m to -6 m: improvement 78%
- From -6 m to -8 m: improvement 61%
- From -8 m to -10 m: improvement 39%
- Below -10 m: improvement negligible < 15%

It is observed an important improvement of the first 6 meters. However, the influence of the applied dynamic compaction reaches 10 meters.

The results of SPT indicate an increase of the number of blows from 8 – 10 to 20 – 25 blows for a penetration of 30c m.

The graphs from Figure 6.3 and Figure 6.4 show the average cone tip resistance and the average SPT values obtained before and after D.C.

6.3.5 Laboratory tests results

In accordance with the presented methodology were executed the necessary laboratory tests. Table 6.3 presents in synthesis the parameters obtained from the laboratory tests and used for evaluation. These values and their variation in depth are represented also graphically.

As shown, average dry density increased after DC. Before compaction ρ_d = 1.63 g/cm^3 and after compaction ρ_d = 1.75 g/cm^3 (see Figure 6.5). Also, it is shown a reduction of the average porosity from 40% obtained prior to DC to 35% after DC (see Figure 6.6).

The tests on undisturbed samples obtained from the geotechnical borings show an average plasticity of 20% and moisture of 17%.

Double oedometer tests on undisturbed samples were performed in order to determine the additional settlement, the structural resistance and the oedometer modulus. As a result we have:

- Average structural resistance before the improvement is about 130 kPa.
- Reduction of the additional settlement index (i_{m300}) from 2.37% (maximum i_{m300} = 4.72%) before the improvement to 0% after the improvement (Figure 6.7).
- In natural state and moisture, the average odometer modulus calculated between the load steps 200 and 300 kPa before dynamic compaction is $M_{200\text{-}300before}$ = 11,100 kPa and the modulus after the improvement is $M_{200\text{-}300after}$ = 16,000kPa (see Figure 6.8)
- At saturation, the deformation modulus becomes about double after DC; from a value of $M_{200\text{-}300before}$ = 6,300kPa increases to a value of $M_{200\text{-}300after}$ = 12,000kPa (see Figure 6.9).

In addition, on compacted samples were performed direct shear tests type U.U. (Unconsolidated – Undrained) and C.U. (Consolidated – Undrained). The samples were taken from two locations, at different depths. The results are presented in Table 6.3.

Are observed average values at natural moisture for friction angle of $\varphi = 26^o$ and cohesion of c = 51 kPa for C.U. and $\varphi = 18^o$ and c = 50 kPa for U.U. At saturation the average friction angle is $\varphi = 23^o$ and the average cohesion is c = 20 kPa for C.U.

6.3.6 Certification of loess improvement

Analyzing the data obtained before DC application the natural soil until 6 m has the following properties:

- the soil is cohesive, generally yellow clayey silt, rarely with limestone concretions and with fraction of silt (d = 0.002 – 0.062 mm) in proportion of 47 – 60%
- under unsaturated conditions, S_r = 0.5 – 0.8
- the natural porosity is n = 34 – 46%
- the dry density on natural soil has values of values ρ_d = 1.45 – 1.76 g/cm^3

- i_{m300} has values from 1 – 5% resulting an average of i_{m300} = 2.37%; generally, i_{m300} is greater or equal with 2 %

Taking into consideration the above, the analyzed loess deposit in natural state is classified as sensitive for saturation conditions.

After improvement, the compacted material satisfies the criteria established in order to consider that loess is no longer sensitive at saturation:

- reduction of porosity n = 31 – 40%, therefore $n \leq 40\%$
- increasing of the dry density ρ_d =1.63 – 1.84 g/cm^3, therefore $\rho_d > 1{,}6$ g/m^3
- decreasing of the specific additional settlement index i_{m300} = 0 – 2,4%, therefore $i_{m300} < 2\%$
- increasing the average oedometer modulus at natural moisture $M_{200\text{-}300nat}$
- increasing the average oedometer modulus at saturation $M_{200\text{-}300sat}$

The conditions established in order to certify the quality of the works are satisfied as following:

- $i_{m300comp} / i_{m300nat} = 0.18 < 1$
- $\rho_{dcomp}/\rho_{dnat} = 1.07 > 1$
- $n_{com} / n_{nat} = 0.90 < 1$
- $M_{200\text{-}300\ com} / M_{200\text{-}300\ nat} = 1.43 > 1$
- $M_{200\text{-}300\ comsat} / M_{200\text{-}300\ natsat} = 1.91 > 1$

The ratios of the average values obtained before and after compaction are presented also in Table 6.5. Moreover, in Table 6.6 it is shown that the values for tip resistance (q_c) after compaction increased over 2.5 MPa.

Considering the above, it is concluded that after DC, the improved loess deposit does not have sensitivity at saturation.

6.4 CONCLUSIONS

Dynamic compaction trials were performed at an experimental site, of approx. 40,000 m^2, located in Constanta area and more specifically at Valul lui Traian in the vicinity of the railway line Bucharest – Constanta. Prior geotechnical investigations revealed the existence of a 12 m thick loess deposit, sensitive to water on the first 6 m.

According to the soil characteristics and construction requirements, was required the treatment of the loess deposit for the first 6 m. In this regard has been applied Dynamic Compaction (DC) technique.
The purpose for applying DC was to improve the bearing capacity of the soil to support the embankments, to reduce differential settlements and to reduce the collapse potential of the loess.

To certify the improvement by dynamic compaction was undertaken a program of various tests, including compaction tests, in situ and laboratory tests. The tests were executed prior to and after DC. The results were processed and interpreted.

From the tests performed on natural soil the loess deposit before improvement is classified as collapsible: average additional settlement index i_{m300} = 2.37%, average porosity of 40%, average dry density of about 1.6, the average cone resistance is 1 – 1.5 MPa.

After the treatment the physical and mechanical parameters improved, as follows:

- The additional settlement is practically eliminated, average i_{m300} = 0.43% (< 2%)
- Reduction of average n to 35% (< 40%)
- Increasing of the dry density average ρ_d = 1.75 g/cm^3 (> 1.6 g/cm^3)
- The odometer modulus increased for both natural moisture and saturation conditions
- The average cone resistance increased q_c = 2.5 – 3.5 MPa (> 2.5 MPa);

Thus, for the compacted ground under conditions of saturation will not occur additional settlements under its own weight and either under external loads. Before compacting, the ground could suffer additional non-uniform settlements with values of 15 – 40 cm. Moreover, is demonstrated a decrease of compressibility reflected by the increase of oedometric modulus.

Based on the presented results, it is concluded that, for a depth of 6 meters, the dynamic compaction program has achieved the project requirements. Therefore, the improved loess deposit can be certified as non-collapsible and it can be categorized as good foundation soil.

Table 6.1: Energy Parameters

Phase	Number of Blows	Height (m)	Pounder (T)	Grid (m^2)	Area (m^2)	Energy (tm/m^2)
1st Phase	12	23	18	49	-	101.4
	14	23	18	49	-	118.3
2nd Phase	12	23	18	49	-	101.4
	14	23	18	49	-	118.3
Ironing LBR 855	2	20	18	-	3.8	189.5
Ironing LBR 843	4	14.5	14	-	4.8	169.2
Total Energy*						**392**
Total Energy**						**426**
Total Energy ***						**372**
Total Energy****						**406**
Observation:	*	12 blows x 23 m x 18 T + Ironing LBR 855				
	**	14 blows x 23 m x 18 T + Ironing LBR 855				
	***	12 blows x 23 m x 14 T + Ironing LBR 843				
	****	14 blows x 23 m x 14 T + Ironing LBR 843				

Table 6.2: Summary of crater and platform measurements

Phase	Average energy (tm/m^2)	Crater Volume (m^3)	S_{DC} (cm)	Efficiency ratio ($cm/tm/m^2$)	Volume reduction (%)
1	110	12.60	24	0.22	3
2	110	12.89	19	0.17	2.3
Ironing	179	-	33	0.18	4.1
TOTAL	**399**	**-**	**76**	**-**	**9.4**

Table 6.3: Parameters obtained from laboratory tests

Depth (m)	In natural soil							In compacted soil						
	i_{m3} (%)	I_c	Average e	Average ρ_d	Average n	M_{2-3} natural (kPa)	M_{2-3} saturated (kPa)	i_{m3} (%)	I_c	Average e	Average ρ_d	Average n	M_{2-3} natural (kPa)	M_{2-3} saturated (kPa)
0.60			0.67	1.63	39.96					0.48	1.84	32.51		
1.50			0.6	1.71	37.31					0.61	1.69	37.73		
1.80			0.52	1.76	34.20			0.1	0.81	0.52	1.79	34.30	21462	12683
2.40	4.72	0.78	0.85	1.45	46.04	7848.2	3455.5	0	0.97	0.49	1.82	32.99	12440	10769
3.00			0.65	1.65	39.45					0.45	1.87	31.12		
3.60	2.51	0.78	0.87	1.47	45.84	9753.5	5008.3	0	0.88	0.62	1.68	38.24	15993	11340
4.20			0.63	1.67	38.51			0	0.83	0.67	1.63	40.12	12621	14548
4.80	1.76	0.94	0.61	1.67	37.72	14548	7035.2	0	0.77	0.58	1.72	36.69	17170	13482
5.40			0.53	1.74	34.78					0.51	1.77	33.56		
6.00	0.5	0.97	0.72	1.56	41.72	12381	9827.2	2.45	1	0.64	1.66	39.06	15895	9717
Average	2.37	0.87	0.67	1.63	39.55	11133	6332	0.43	0.88	0.56	1.75	35.63	15930	12090

Table 6.4: Direct Shear Tests in compacted soil at different moisture

Location	Test type	Depth (m)	NATURAL		SATURATED	
			φ^o	c (kPa)	φ^o	c (kPa)
1	C.U.	2.7	27.5	42.8	20.42	21.9
		2.5	29.46	22.5	26.14	18
		Average	28.48	32.65	23.28	19.95
2	U.U.	2.2	16.4	47.9	-	-
		2.7	19.54	52.6	-	-
		Average	17.97	50.25	-	-
	C.U.	1.5	22.51	83.9	-	-
		2.5	24.11	72.6	-	-
		5.5	23.29	51.5	-	-
		Average	23.30	69.33	-	-

Table 6.5: Ratios of the average values obtained before and after compaction

i_{m3} (%)	I_c	Average e	Average ρ_d	Average n	M_{2-3} natural (kPa)	M_{2-3} saturated (kPa)
0.18	1.01	0.84	1.07	0.90	1.43	1.91

Table 6.6: Values of the tip resistance after compaction

No.	CPT	Average q_c (MPa)		
		0 - 2 m	2 - 5 m	5 - 6 m
1	CPT 1A	2.1	2.1	1.4
2	CPT 2A	3.8	2.6	2
3	CPT 3A	4.2	2.5	2
4	CPT 4A	1.9	2.1	1.5
5	CPT 5A	3.5	2.5	1.5
6	CPT 6A	3.9	2.5	1.9
7	CPT 7A	4.2	3.3	2.6
8	CPT 8A	3.5	2.9	3.9
9	CPT 9A	5.7	3	3.1
10	CPT 10A	3.5	2.7	2.4
11	CPT 11A	2.9	2.2	2.3
12	CPT 12A	4.3	3	3.6
13	CPT 13A	4	4.8	4.5
14	CPT 14A	4	4.4	4
15	CPT 15A	2.8	2.7	2.1
Average values for all the area		**3.62**	**2.89**	**2.59**

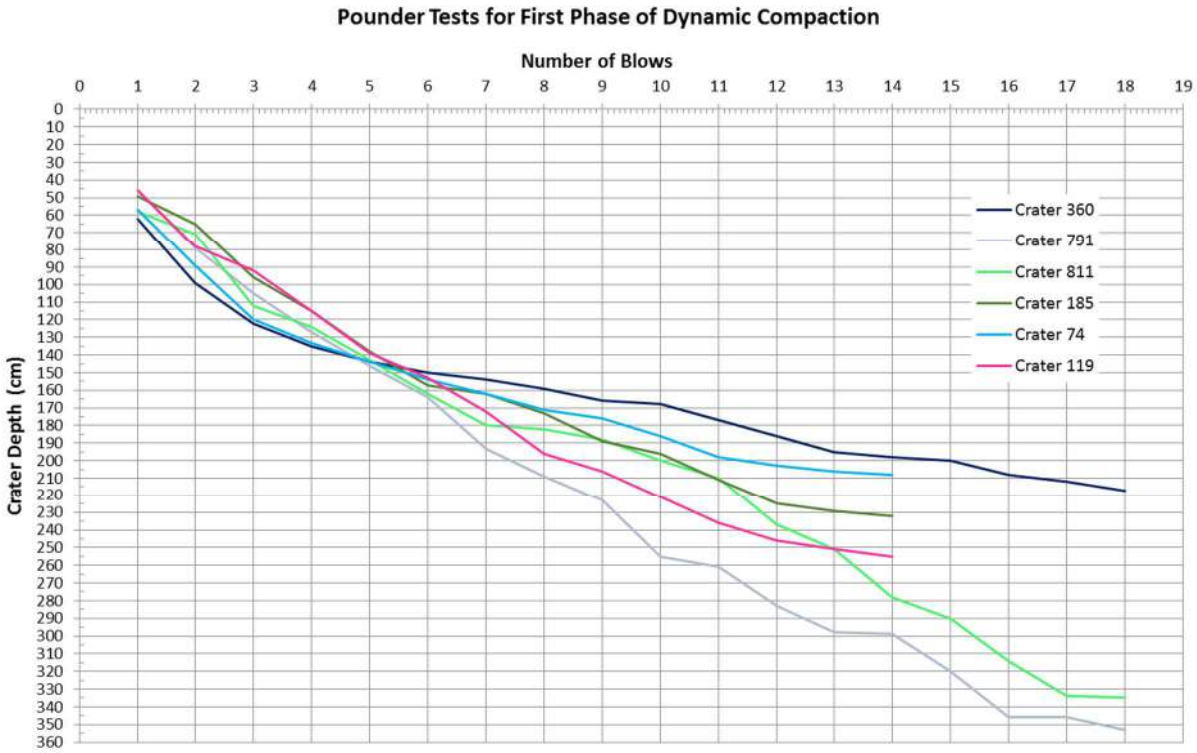

Figure 6.1: Pounder Tests for first phase of DC

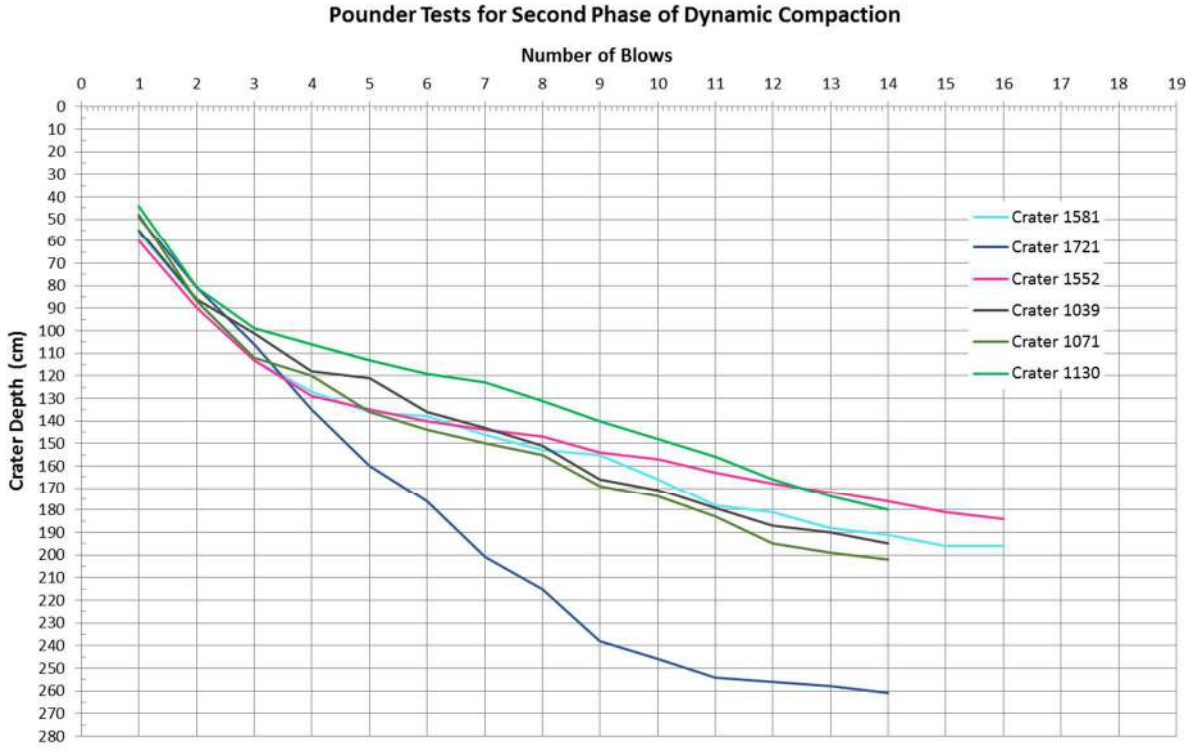

Figure 6.2: Pounder Tests for second phase DC

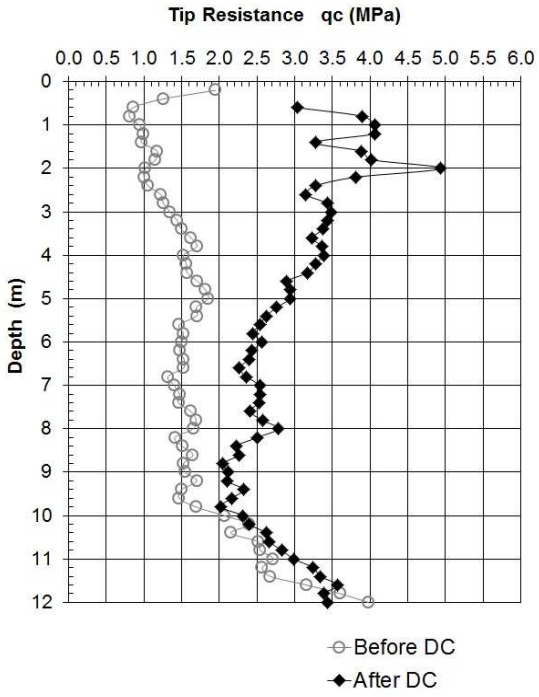

Figure 6.3: Average cone tip resistance with depth

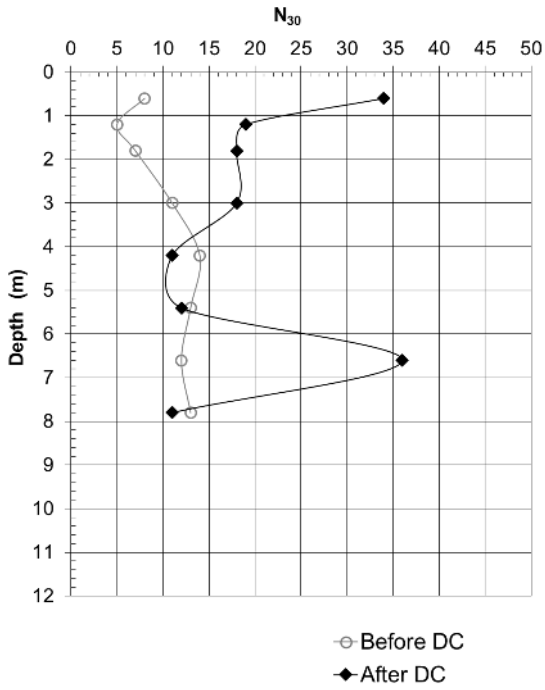

Figure 6.4: SPT Profile

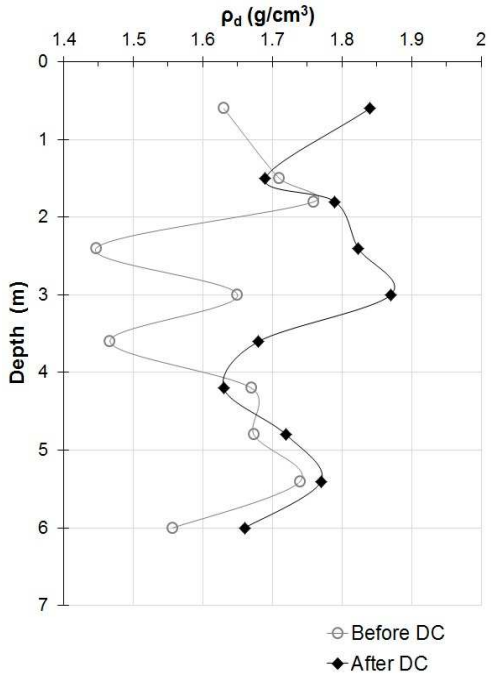

Figure 6.5: Average dry density with depth

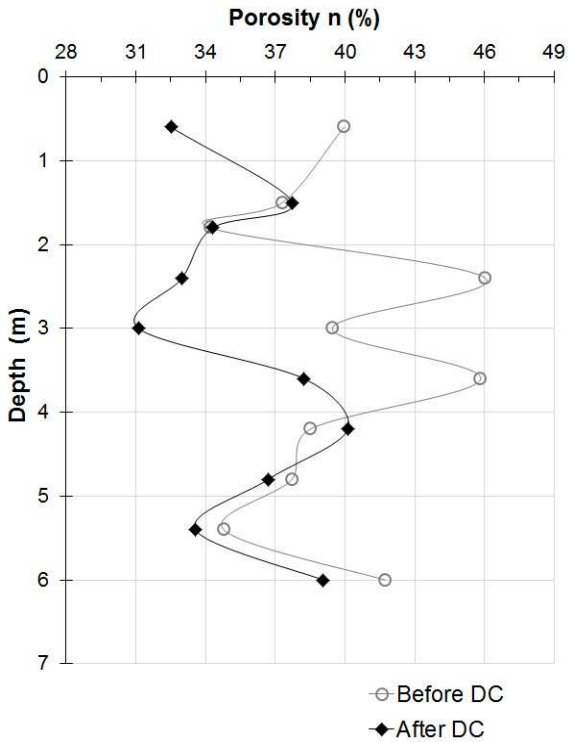

Figure 6.6: Average porosity with depth

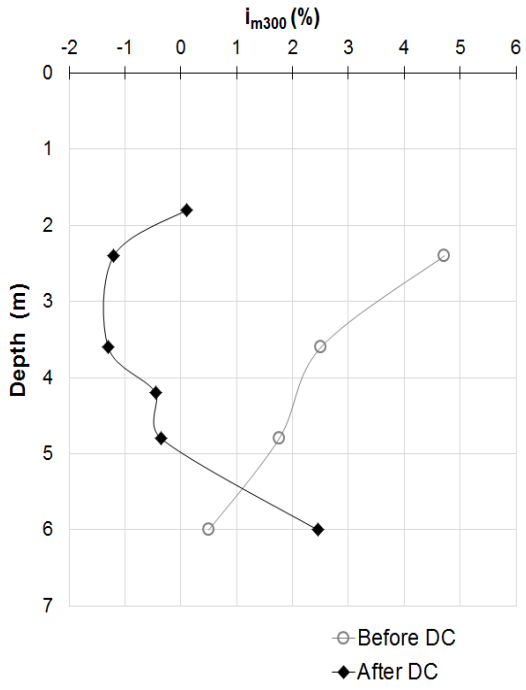

Figure 6.7: Average additional settlement index with depth

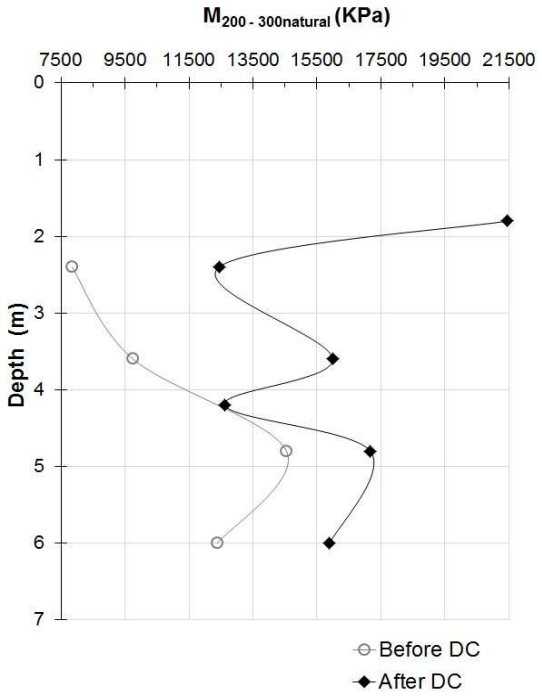

Figure 6.8: Average oedometer modulus at natural moisture with depth

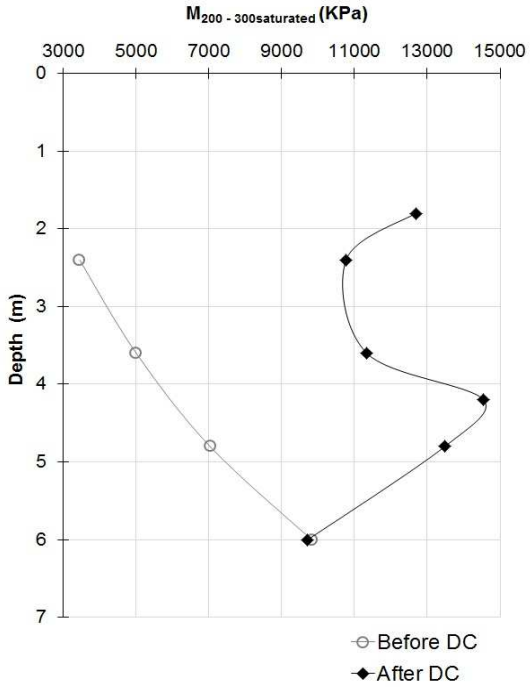

Figure 6.9: Average oedometer modulus at saturation with depth

CHAPTER 7: NUMERICAL ANALYSIS

7.1 INTRODUCTION

The present chapter summarizes the steps for the development of a simple numerical tool for the simulation of the Dynamic Compaction (DC) at the experimental site. The particular tool was developed using the commercially available Finite Difference Code FLAC v5.0 and a simple soil model, which was employed for the description of the soil response. The ultimate objective is to use the previous numerical tool for a selected "typical" site that is part of the experimental site. In the specific site, the dynamic compaction ground improvement method was applied for the improvement of the encountered soil conditions.

The numerical tool's predictions are compared against the recorded field results so that its efficiency is evaluated. Additionally, given the simplicity of the employed soil model, it is clearly stated, which aspects of the field behavior are captured and which ones are not properly simulated. For that reason, recommendations for improvements are also made based on the lessons learned from this study.

7.2 BRIEF DESCRIPTION EXPERIMENTAL SITE

The main aspects of the selected case history with regards to the location of the site, site investigation and soil properties as well as the executed dynamic compaction are provided in the present paragraph.

7.2.1 DC Execution

DC execution is presented in details in Chapter 6.

7.2.2 Site Investigation and Soil Properties

There were performed 15 Cone Penetration Tests (CPT) and 2 Standard Penetration Tests (SPT) as shown in Figure 7.1.

Soil Properties.- for this study 1-D constrained modulus M was estimated using the following empirical relationship:

$$M = 5 * q_c \,(\text{MPa}) \qquad \textit{Eq. 7-1}$$

Young's modulus was subsequently calculated based on the following Eq. 7-2 assuming a Poisson's ratio ν equal to 0.25:

$$M = E\frac{(1-\nu)}{(1+\nu)(1-2\nu)} \qquad \textit{Eq. 7-2}$$

Bulk and shear modulus are estimated based on Eq. 7-3 and Eq. 7-4:

$$B = \frac{E}{3(1-2\nu)} \qquad \textit{Eq. 7-3}$$

$$G = E\frac{(1-2\nu)}{2(1-\nu)} \qquad \textit{Eq}. 7\text{-}4$$

The calculated stiffness properties with depth before and after improvement are provided in Figure 7.4. Uniform stiffness was used as input in the analyses to reflect the before improvement conditions, and based on Figure 7.4, the average stiffness properties were set equal to:

- Young's modulus: E = 7,000 kPa
- Bulk modulus: B = 4,700 kPa
- Shear modulus: G = 2,800 kPa

The calculated stiffness properties after dynamic compaction are also illustrated in Figure 7.4and are on average equal to:

- Young's modulus: E = 11,000 kPa
- Bulk modulus: B = 7,365 kPa
- Shear modulus: G = 4,420 kPa

Based on the above, and following the same process described earlier, soil stiffness properties before dynamic compaction were calculated equal to:

- Young's modulus: E = 3,640 kPa
- Bulk modulus: B = 2430 kPa
- Shear modulus: G = 1460 kPa

Initial friction angle of the material is reportedly equal to 17 degrees based on evaluation of available soil investigation reports, while cohesion is estimated equal to 15 kPa. We also estimated friction angle based on the empirical correlation proposed by Kulhawy and Mayne (1990) shown in Eq. 7-5:

$$\varphi' = 17.6° + 11° \log(q_{ti}) \qquad \textit{Eq. 7-5}$$

in which $q_{ti} = \dfrac{\dfrac{q_t}{\sigma_{atm}}}{\left(\dfrac{\sigma'_{vo}}{\sigma_{atm}}\right)^{0.5}}$ is the stress normalized tip resistance ($\sigma_{atm} = 98.1$ kPa).

The resulting friction angle profile with depth is presented in Figure 7.5, from which it is concluded that friction angle is on average equal to 30 degrees, a significantly greater value. Note that the Kulhawy and Mayne (1990) equation was developed for clean sands, and thus, may not be appropriate for these deposits. However, this value was also considered a possible reasonable estimate for the effective friction angle of the deposits.

In addition, based on Table 7.1 and
Table 7.2, and the SPT data presented in Figure 7.3, friction angle is estimated between 29 – 35 degrees. Thus, a value of 30 degrees was considered in the parametric analyses.

7.3 METHODOLOGY OF SIMULATION

7.3.1 Description of Numerical Methodology

In the subsequent sections, the main assumptions of the numerical methodology are outlined.

Mesh discretization. Simulation of dynamic compaction is performed using axisymmetric conditions, through 2-dimensional (2D) numerical analyses. The general outline of the modeling space is illustrated in Figure 7.6. In terms of mesh discretization, in the vicinity of the pounder, 0.1×0.1 m zones are defined and the particular zone size is increased with depth and horizontal distance from the pounder up to 0.2×0.2 m at the edges of the configuration. This discretization was verified to be adequate based on sensitivity analysis.

Pounder simulation. Based on the provided pounder dimensions shown in Figure 7.2, the effective area is equal to 3.8 m^2. The pounder was simulated as an elastic rigid body on the top of the grid, illustrated in Figure 7.6, with a width equal to 1.0 m, upon which the velocity (loading) time history was applied. As specified in FLAC, the effective radius is estimated as the radius to the point midway between the last grid-point with an applied velocity and the adjacent grid-point. Hence, the effective radius of the circular pounder equals 1+0.1/2 = 1.05 m, this corresponding to an area equal to $\pi*R^2 = 3.5$ m^2. The particular pounder area is roughly 9% lower than the actual one. Moreover, the pounder is assigned properties of steel, i.e., a mass density equal to ρ=7.85 Mgr/m^3, Young's modulus equal to E_s=200,000 kPa, and Poisson's ratio equal to v=0.2, resulting in calculated bulk modulus equal to B=166,667 kPa and shear modulus equal to G=76,923 kPa.

Loading sequence. Consists of a series of triangular pulses, of period T and a maximum impact velocity (imp_vel), as it is also illustrated in Figure 7.7. Recurrent pulses are separated by intervals of zero loading (break) of user-specified duration. The loading sequence is programmed in FISH language within the input data file. Hence, the characteristics of the input motion, namely the period of the pulse (***T***), the interval between consecutive tamper drops (***break***), the impact velocity due to the dropping weight (***imp_vel***), can be easily modified by the user to simulate different loading conditions. The number of tamper drops is also specified by the user. Note that the total time interval was selected to be 1 sec, this being an adequately long period of time for the dissipation of input energy between consecutive blows during the dynamic analyses. Larger values of interval time can be used without any impact on the results of the analyses. In reality, the interval time between two consecutive drops is significantly longer and in the order of 25-30 seconds. However, the computational cost involved in the consideration of such a long time interval of zero loading would unnecessarily result in increased calculation time for the execution of such numerical analyses. The results of the analyses are independent of duration of the "break".

Modeling impact/Energy Input. The recurrent loading input due to the impact of the pounder is simulated by applying a velocity time history upon the rigid body described earlier. The magnitude of the specific time history is initially computed based on the following equation describing the free fall of the pounder from a specific height:

$$imp\_vel = \sqrt{2gh} \qquad \textit{Eq. 7-6}$$

Hence, given a specific drop height, the maximum velocity magnitude is computed. For a drop height (h) of 23 m, as specified in Error! Reference source not found., the impact velocity is computed equal to imp_vel=21.24 m/s.

Prescription of a constant impact velocity results in a prescribed input displacement time history (equal to the area of the velocity pulse). In other words, the integral of the applied velocity time history will be equal to the input displacement applied at the ground surface. As a result, by prescribing a vertical velocity time history for the tamper, the evolution of the dynamic vertical displacement of the tamper is defined and is linear. The impact pulse was modeled as a triangular load and a period of T=0.1 sec was selected based on sensitivity analyses. The velocity amplitude of the triangular load was adjusted so that the displacement time history of the computed impact velocity and the triangular load with T=0.1 sec is the same.

The final loading time history used in the analyses is presented in Figure 7.7 and consists of 20 tamper drops of period T = 0.1 sec, separated by a break time of 1sec, and an amplitude of 2.12 m/sec.

Damping. Local non-viscous damping is considered throughout the grid configuration and, in the absence of available data, was assigned a typical value of 5%. Parametric analyses were also performed to assess the results for larger and smaller amounts of damping. The central idea behind local damping is that mass is added to a grid point when velocity changes sign and subtracted when it passes a maximum or minimum point. There is overall conservation of mass, because the amount added is equal to the amount subtracted. Hence, increments of kinetic energy are removed twice per oscillation cycle (at the velocity extremes).

Boundary Conditions were different during the generation of initial geostatic stresses and the subsequent loading of the soil surface. Namely, for the generation of geostatic stresses, horizontal displacements are restrained along the lateral boundaries, whereas restriction of vertical movement is imposed along the vertical direction at the bottom boundaries, thus allowing the undisturbed development of settlements. The bottom boundaries were not restrained in the horizontal direction, in order to avoid the generation of parasitic shear stresses.

During dynamic loading, fixity conditions were changed, and a sensitivity analysis was carried out aiming in specifying a suitable boundary condition scheme. Given the axi-symmetric nature of the problem, the application of the free-field boundary conditions provided in FLAC was not possible. Hence, quiet boundaries were initially considered at the edge of the model space, while the grid points along the base were kept fixed in the horizontal and vertical directions.

The above type of boundary conditions is illustrated in Figure 7.8 In the sequel, quiet boundaries were removed and along the vertical boundary of the configuration “roller” type boundaries were considered, as presented in Figure 7.9.

The effect of the two different types of boundary conditions is appraised in Figure 7.10**,** in terms of generated volumetric strains after 20 tamper drops. It is shown that quiet boundary conditions, introduce some disturbance, mainly at the edges of the configuration, and especially for increasing number of drops. In general, however, for practical purposes, the two boundary conditions did not affect the results of this study. In the sequel, for the execution of the parametric investigation, the roller-type boundary conditions are selected.

Soil model. The Mohr-Coulomb constitutive model is used to define the failure state. The required soil model parameters are: (i) bulk modulus (kPa), (ii) shear modulus (kPa), (iii) friction angle (deg) and (iv) cohesion (kPa). For the baseline analysis, the soil model parameters were set equal to the values estimated before the execution of dynamic compaction. These are summarized in the first column of

Table 7.3. To investigate the effect of stiffness and strength, the considered soil parameters are marked in red in the second and third columns of the table. Note that in this model, the soil parameters remain constant, i.e., they do not change during the analyses. In reality, soil densification during dynamic compaction will result in an increase in stiffness and strength.

7.3.2 Evaluation of Numerical Results

Numerical results are shown in terms of volumetric and shear strain contours, as well as in terms of the developing strains with depth and number of drops.

Baseline analysis. Contours of volumetric and shear strains at different stages of dynamic compaction, namely the 1st, 5th, 10th, 14th and 20th drop, are presented in Figure 7.11 and Figure 7.12 respectively

- *Strain evolution*
  Shear strain evolution illustrated in Figure 7.11, indicates the occurrence of excessive shearing in the vicinity of the impact zone. Shear strains (1% or higher) appear to be extending up to a depth of about 5.0 m and a width reaching up to 3 m.

  The volumetric strain bulb evolution, presented in Figure 7.12 indicates the gradual propagation of the performed compaction to comparable depths with increasing number of drops. Compressive strains accumulate in the soil below the contact area with the tamper, whereas, some heave (i.e. negative volumetric strains based on the sign convention in geotechnical engineering) start developing at the edge of the tamper already from the first drop. The area where significant compressive strains occur reaches a width almost twice the radius of the tamper i.e. 2.0 m approximately and depths in the order of 4 meters.

- *Strain distribution and depth of improvement*

Volumetric and shear strain distribution with depth along the axis of the configuration (i.e. at the center of the pounder) are presented in Figure 7.13 with volume compression shown as positive. The model predicts the generation of significant volumetric strains upon the first drop, however the particular changes do not increase further after the 5th drop (at the tamper center). Shear strains develop at greater depths than volumetric strains, which should not be surprising for the model used.

- *Depth of improvement*
  It is evaluated based on the shearing and volumetric strain distribution.. At this stage, the soil model that is used to simulate soil response does not allow an update of soil properties based on the induced volumetric or shear strain changes. As a result, it becomes difficult to assess the level of volumetric or shear strain that will result in observed changes in penetration resistance. In this study, it was assumed that volumetric strains in the order of 1% are used as the criterion to define the depth of improvement, the hypothesis being that 1% strain is a large level of strain for most soils. Shear strains can also be used as a criterion.

Based on the above (1% volumetric or shear strain), depth of improvement is equal to approximately 5 m (4-6 m), which is in relatively good accordance to the 7 m predicted based on the empirical Eq. 7-7:

$$D = n\sqrt{WH}$$ *Eq. 7-7*

Where:

- **n** = 0.35 – 0.40 for impervious deposits (primarily clayey soils)
- **W** = weight of the tamper (tons)
- **H** = drop height (m)

Effect of soil properties were evaluated by considering the values for the various soil model parameters summarized in
Table 7.3. Numerical predictions were evaluated in terms of the developing volumetric and shear strains. The results are summarized in Figure 7.14 through Figure 7.17. Since the displacement time history is prescribed, there is no effect on the accumulating displacement.

Figure 7.14 presents the volumetric strain contours after the 14th drop, for the baseline analysis, as well as the results after reducing the soil stiffness and increasing the soil strength. A reduction in soil stiffness increases the bulb of volumetric strains. For a higher friction angle, the volumetric strain bulb extends deeper. In both cases, greater shear strain values are predicted at a certain depth.

Figure 7.15 summarizes the effect of soil properties on the developing shear strains for the baseline case and the parametric analyses. Reducing the soil stiffness increases the shear strain bulb. For a 1% shear strain, the bulb extends up to 4.5 m in depth and 2.5 m laterally. Soil strength noticeably affects the size of the sheared area underneath the pounder both in depth and laterally.

Figure 7.16 summarizes the volumetric strain distribution with depth along the center of the tamper, where strains reach their maximum value. A reduction in soil stiffness primarily affects the magnitude of developing volumetric strains, whereas the depth of significant strain generation i.e. exceeding 1%, is not considerably affected and is approximately 5 m. Volumetric strains in the baseline analysis reach a maximum value of 8%, as opposed to a magnitude of 10 – 12% in the second case. Increasing soil strength results in much greater volumetric strains, (in the order of 20%), also leading to a deeper depth of influence. Overall, 1% volumetric strain is estimated to be, at 4.0 m depth in the baseline case, almost 4.5 m depth in the case of the lower stiffness, and 5.5 m depth in the case of higher strength.

Figure 7.17summarizes the shear strain distribution with depth along the center of the tamper, where strains reach their maximum value. Soil stiffness does not have a significant effect on either the magnitude or the depth down to which shear strains develop. Soil strength modifies the pattern of the shear strain development, which increases gradually with the number of drops. Additionally, the 1% shear strain contour is located from a 5.0-5.5 m depth in the baseline case, to almost 6.5 m approximately in the case of higher strength.

7.4 FINDINGS AND DISCUSSION

A numerical methodology was developed for the simulation of dynamic compaction at the 40,000 m^2 experimental site, using the available site characterization data. The main assumptions of the numerical methodology were evaluated by performing sensitivity analyses. The results of the numerical analyses are presented. Major results indicate that:

- The simplified model can, in a qualitative sense, predict the impact of the energy input on the local soils. The shape of the volumetric and shear strain contours is generally

reasonable. The model indicates significant changes in the soil (in terms of volume and shear) below the tamper for a prescribed energy input (pulse of a given velocity amplitude and frequency).

- Values for the various parameters of the used model were selected based on a review of the site characterization data. The effect of the soil stiffness and strength on the numerical predictions was examined through sensitivity analysis. The results were evaluated mainly in terms of the developing strains and influence depth. Note also that the results of the analyses are sensitive to the values of the model parameters; hence particular attention is required in their selection.
- The depth of improvement (defined as the depth where the volumetric and/or shear strain reaches a value of 1%) is found to be in the order of 4-6 m for the baseline case, which is comparable to a depth of improvement of 7 m using Eq. 7-7and somewhat lower than the values measured in the field (which varied from 6 m to 9 m). The reason for this bias is associated with two main factors: (a) the limitations of the model, as described subsequently; and (b) potential variations in the material properties.

7.5 LIMITATIONS OF CURRENT WORK

This report summarizes the work performed for the development of a simple numerical methodology for the simulation of the Dynamic Compaction technique at a selected experimental site located in Constanta, Romania. A relatively simple and easy to understand elasto-plastic model was successfully employed and was used to assess which aspects of the field behavior are captured and which ones are not properly simulated. However, certain limitations of the model have been identified and form the basis for recommendations for improvements, as follows:

- The impact of the tamper on the ground was modeled as a velocity pulse with certain amplitude and frequency characteristics. Although this attempt is consistent with earlier efforts to model dynamic compaction, alternative ways to model the impact should be explored that consider the high nonlinear characteristics of the impact and the response of the soil to that type of loading.
- The constitutive elasto-plastic Mohr-Coulomb model used has certain limitations. These include: (a) constant modulus in the elastic region; (b) a simplified way to address damping; and (c) constant soil model parameters that are not updated during the improvement process. Of those, especially item (c) is considered particularly critical.
- Analyses were conducted using an axisymmetric 2D model that essentially models one impact location. A fully 3D model, where multiple passes over an entire area can be modeled, also simulating all intermediate stages. However, this would require considerable computational effort and would make a numerical simulation substantially elaborate, significantly increasing the required computational time. Such a task falls outside the scope of the present report. Additionally, prior to the execution of a generalized analysis with more than one compaction locations, it is important the previously recognized numerical restrictions to be resolved.

Table 7.1: Relationship between φ and N_{SPT} for sands (Peck 1974)

N_{SPT} (blows/ foot)	**Density of Sand**	**φ (degrees)**
<4	Very loose	<29
4 - 10	Loose	29 - 30
10 - 30	Medium	30 - 36
30 - 50	Dense	36 - 41

>50	Very dense	>41

Table 7.2: Relationship between φ and N_{SPT} for sands (Meyerhof 1956)

N_{SPT} (blows/ foot)	**Density of Sand**	**φ (degrees)**
<4	Very loose	<30
4 - 10	Loose	30 - 35
10 - 30	Medium	35 - 40
30 - 50	Dense	40 - 45
>50	Very dense	>45

Table 7.3: Properties considered in the baseline analysis

Soil Property	**Baseline Analysis**	**Effect of Stiffness**	**Effect of Strength**
Bulk Modulus B(kPa)	4660	2430	4660
Shear Modulus, G(kPa)	2796	1456	2796
Friction angle (deg)	17	17	30
Cohesion (kPa)	15	15	15

Note: red values are examined

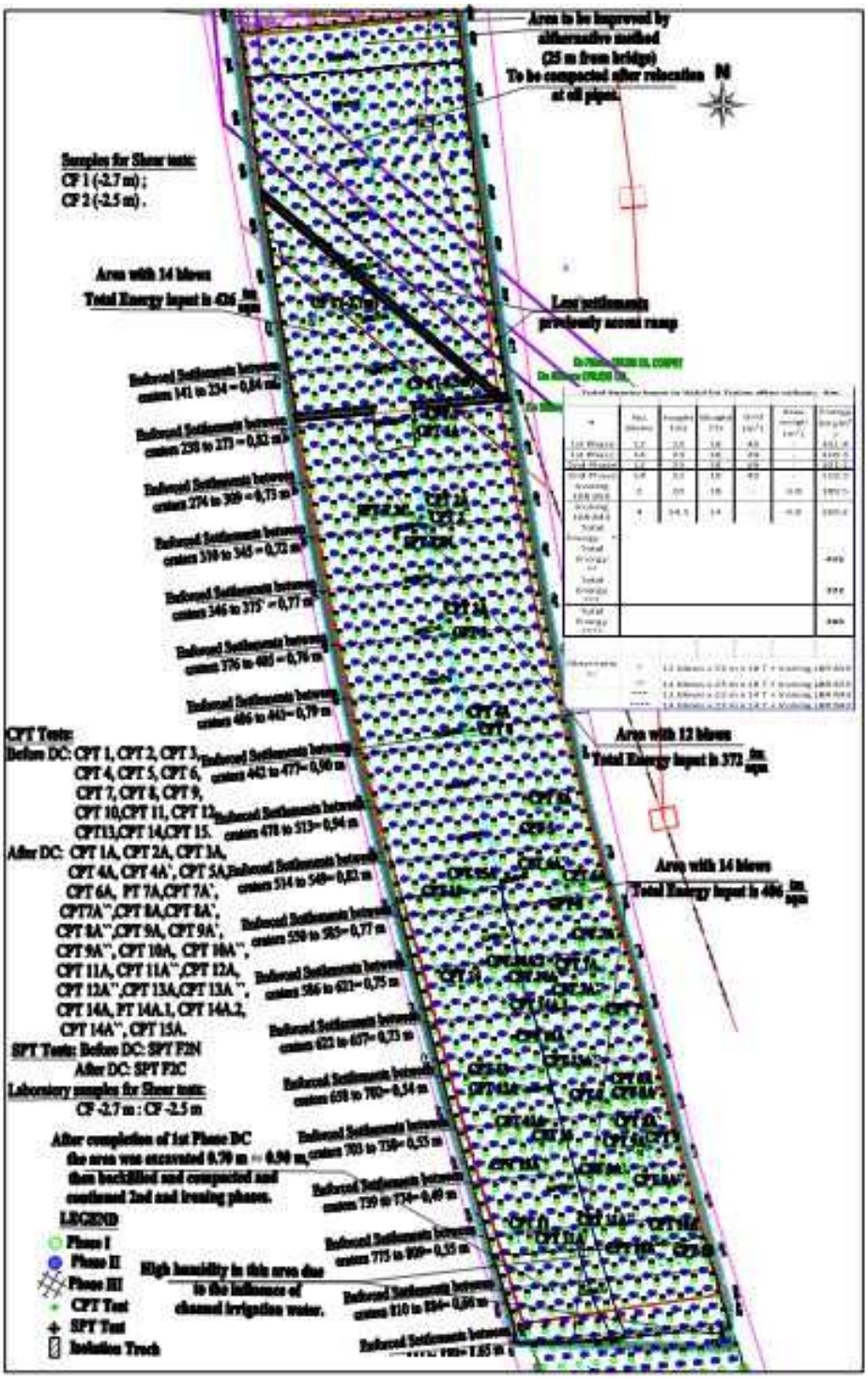

Figure 7.1: Experimental Site Location

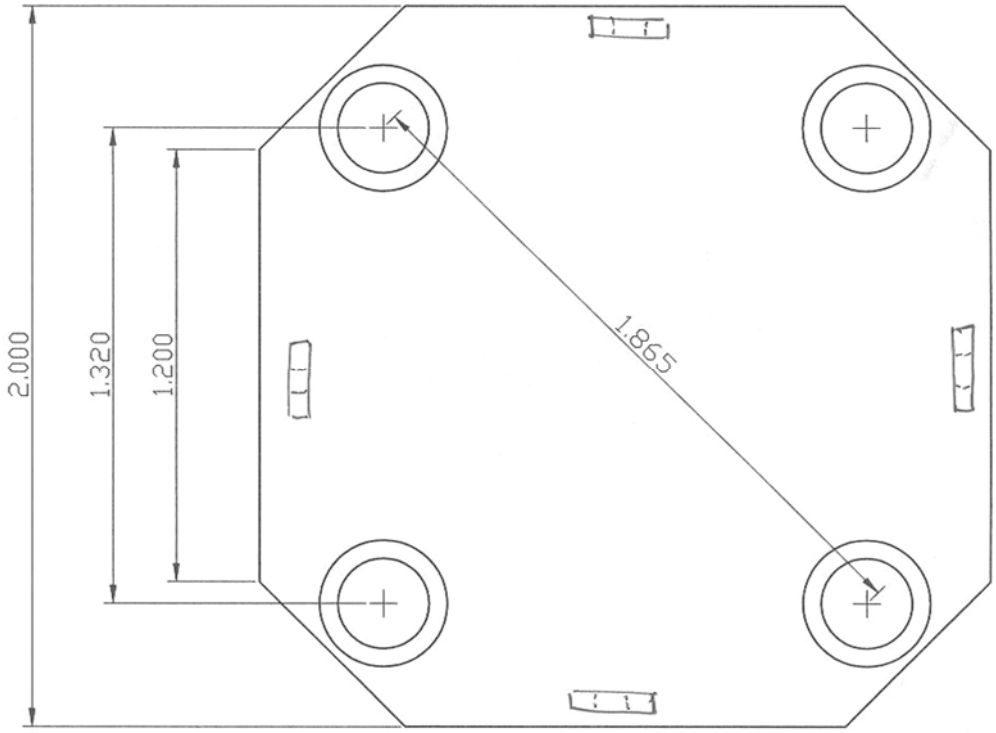

Figure 7.2: Plan dimensions of the steel pounder

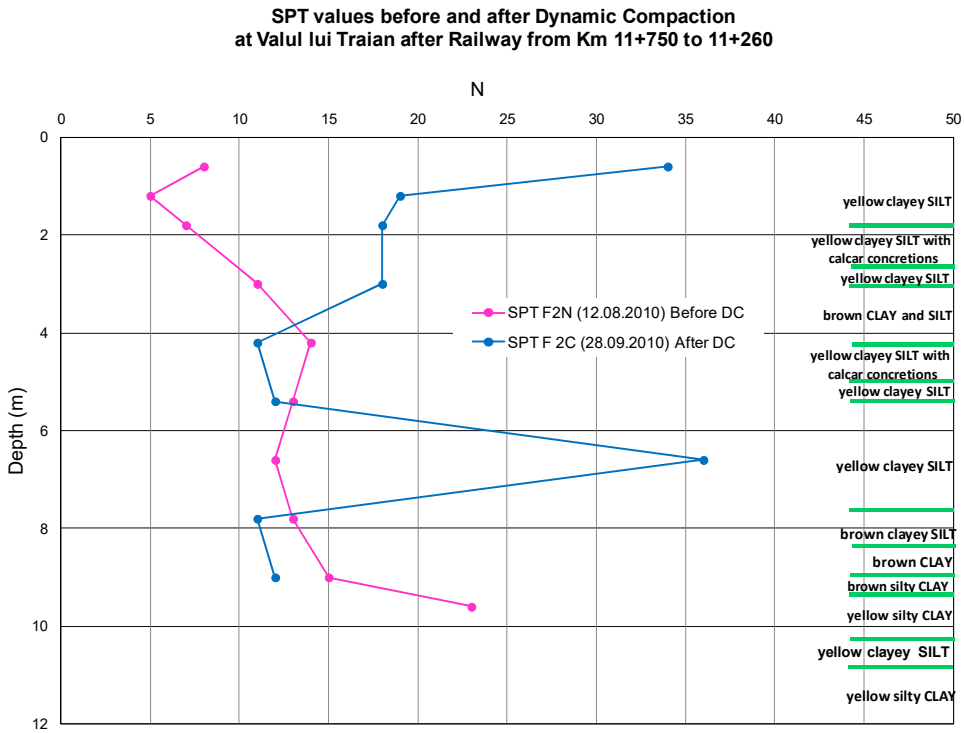

Figure 7.3: N_{SPT} values before and after DC

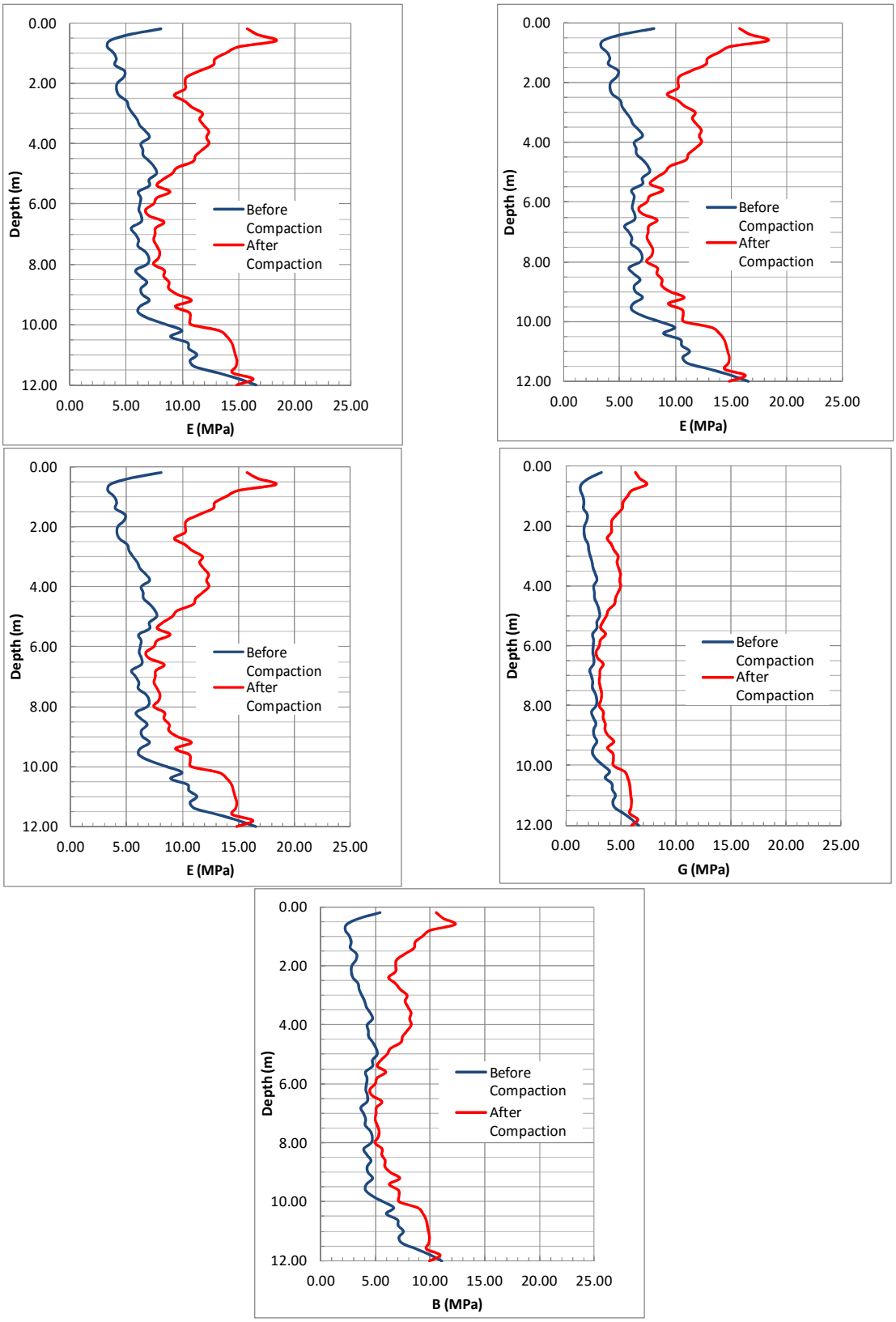

Figure 7.4: Distribution of stiffness properties with depth before and after DC

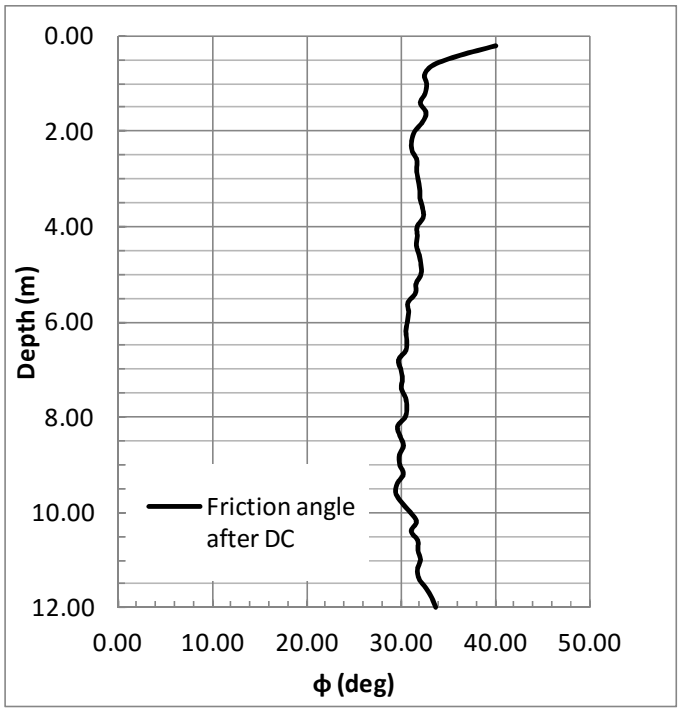

Figure 7.5: Distribution of friction angle ϕ with depth after DC

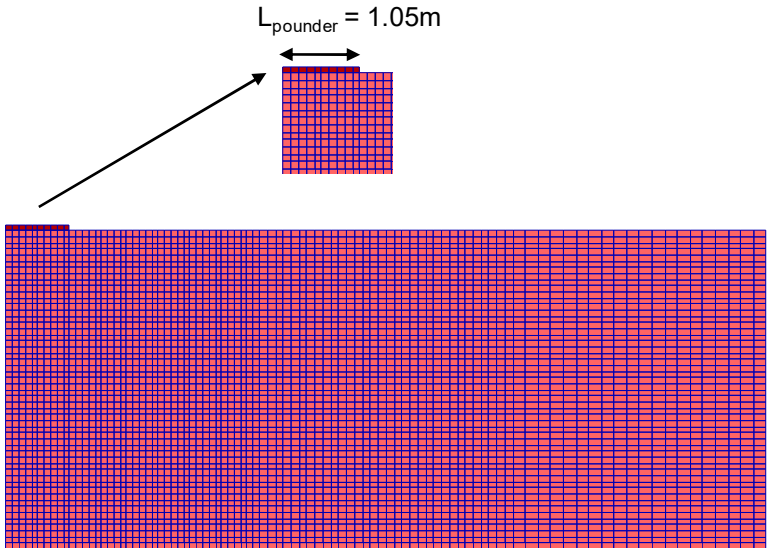

Figure 7.6: Mesh discretization with the pounder simulated as a rigid steel body

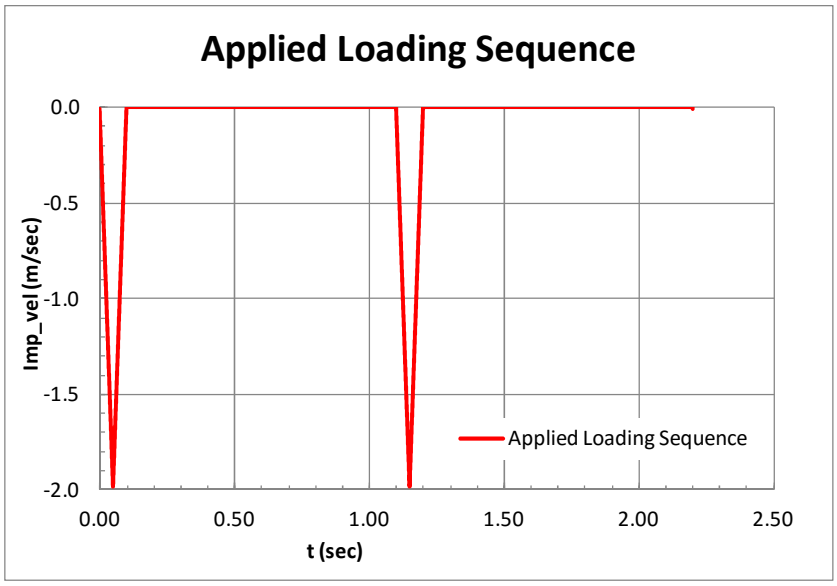

Figure 7.7: Applied loading sequence

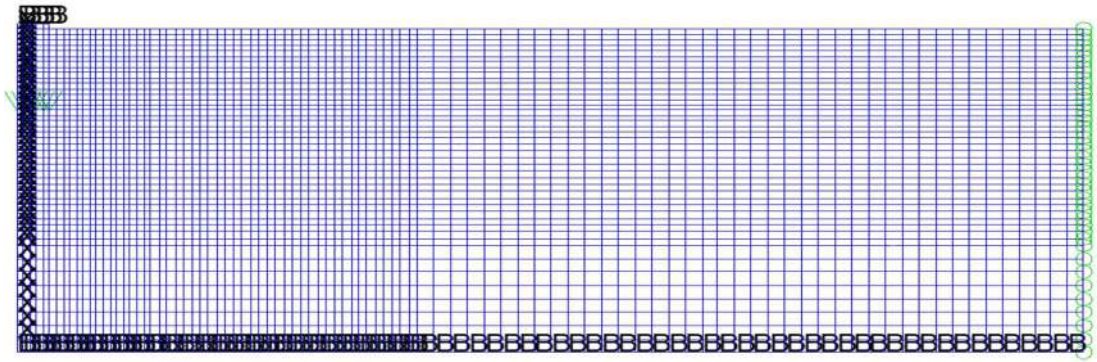

Figure 7.8: Fixed base and quiet boundaries on the left side

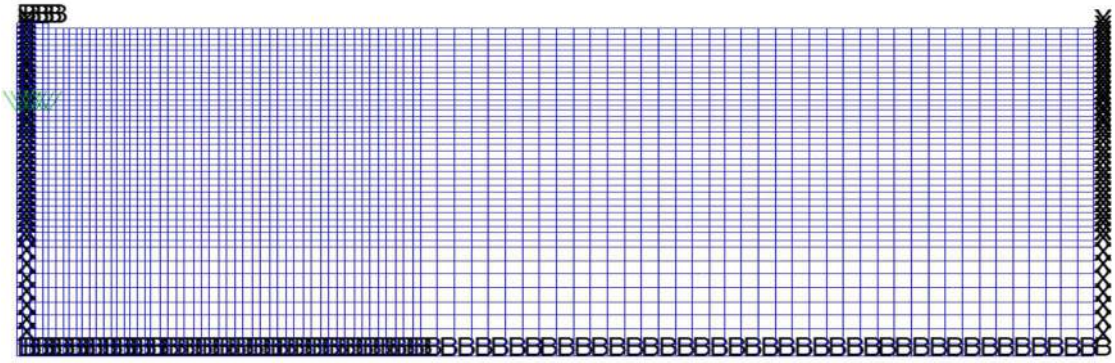

Figure 7.9: Fixed base and “roller” type boundary conditions at the edge

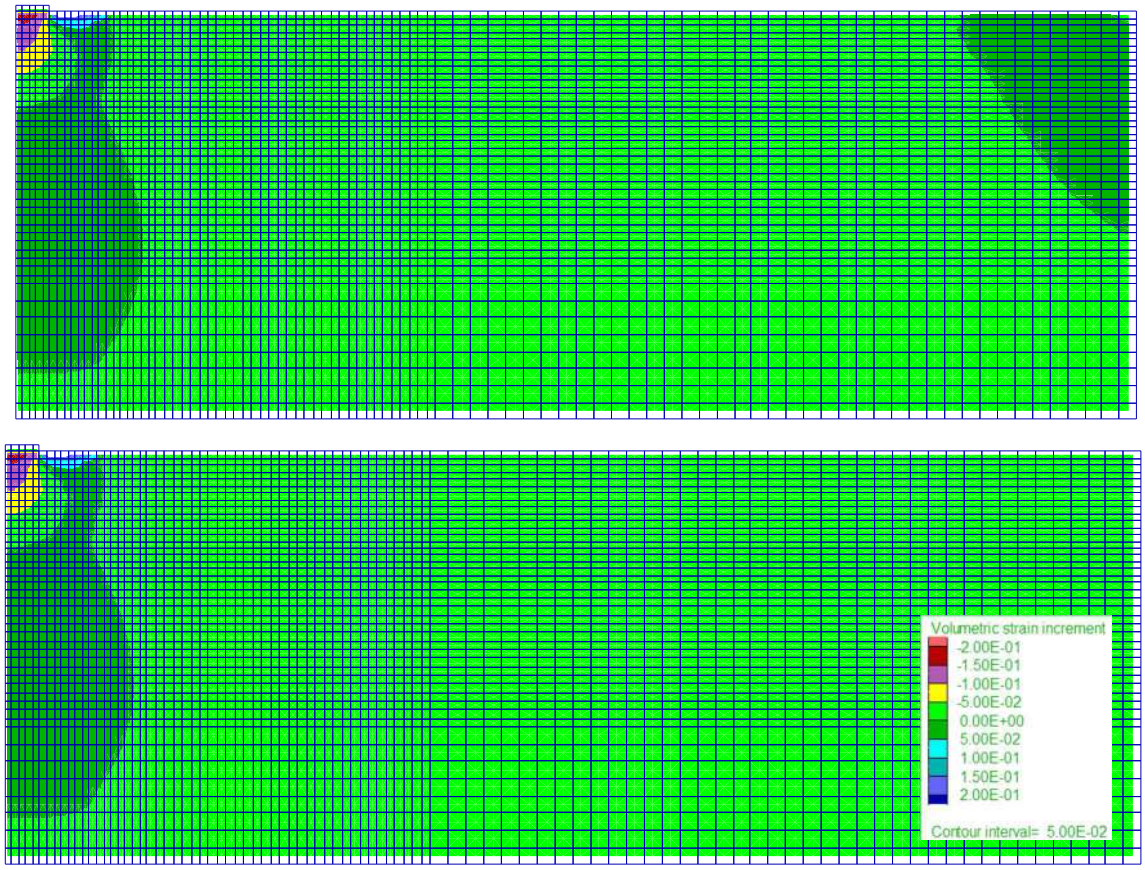

Figure 7.10: Effect of boundary conditions on volumetric strains after 20 drops

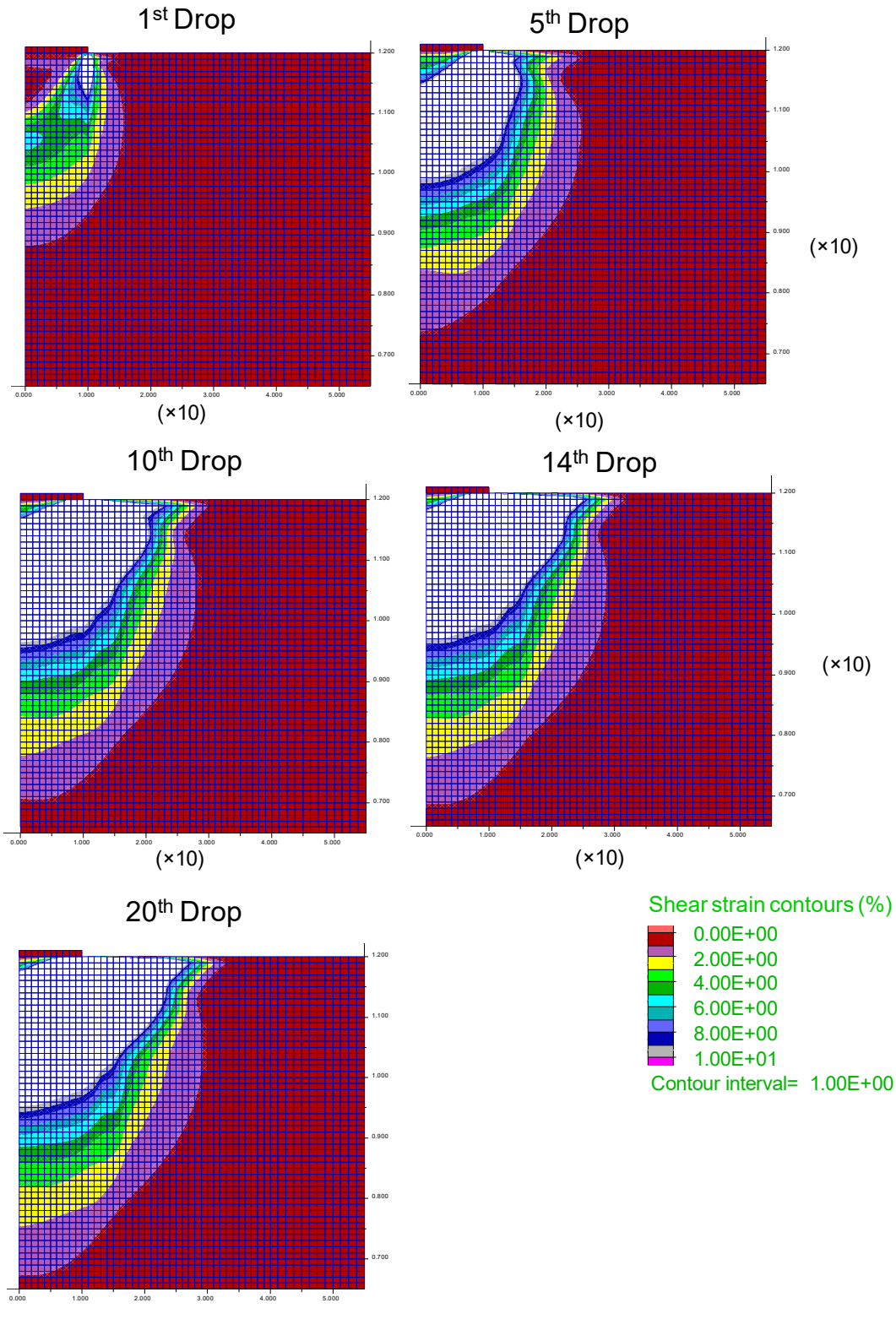

Figure 7.11: Shear strain contours at different number of drops

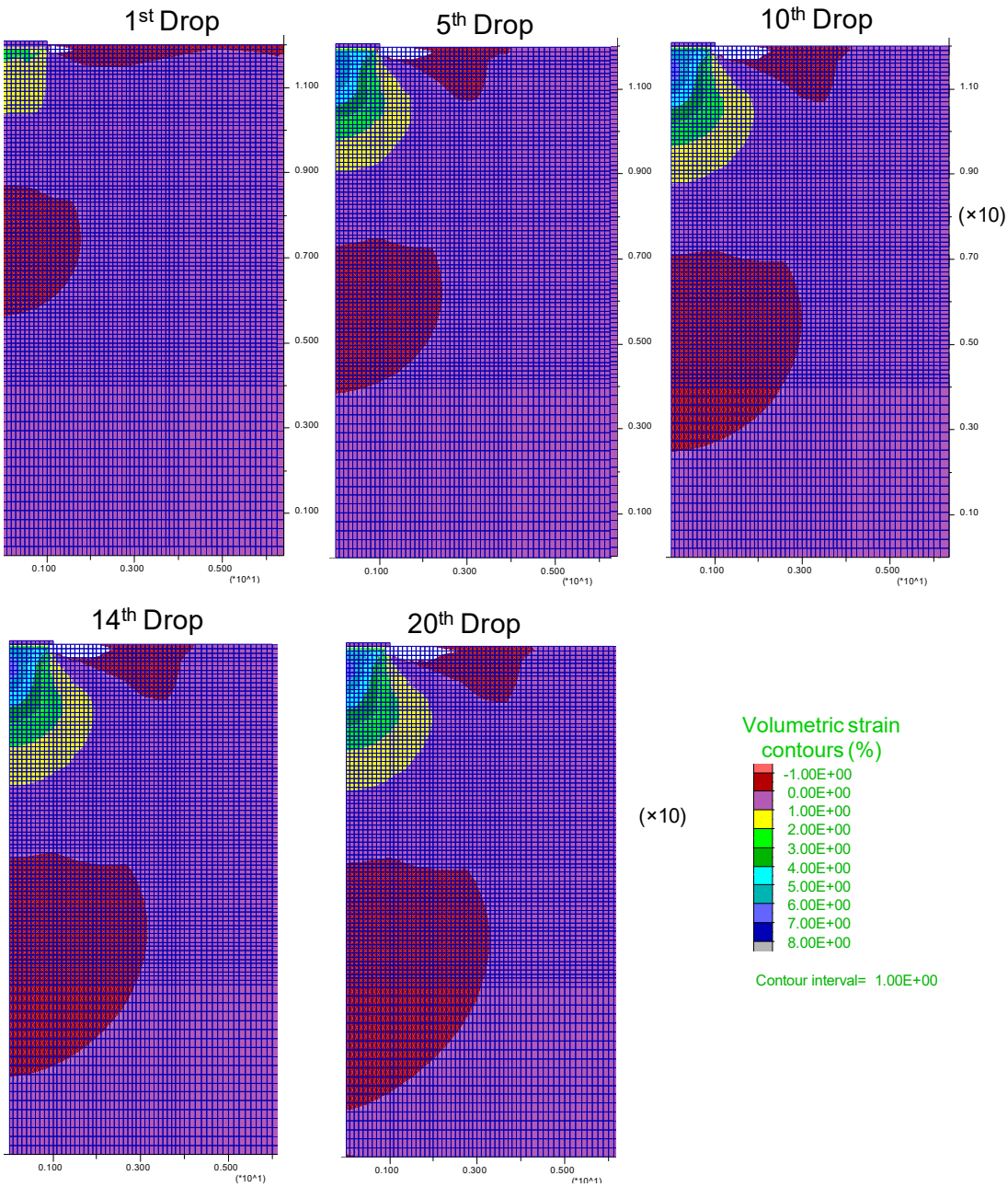

Figure 7.12: Volumetric strain contours at different number of drops

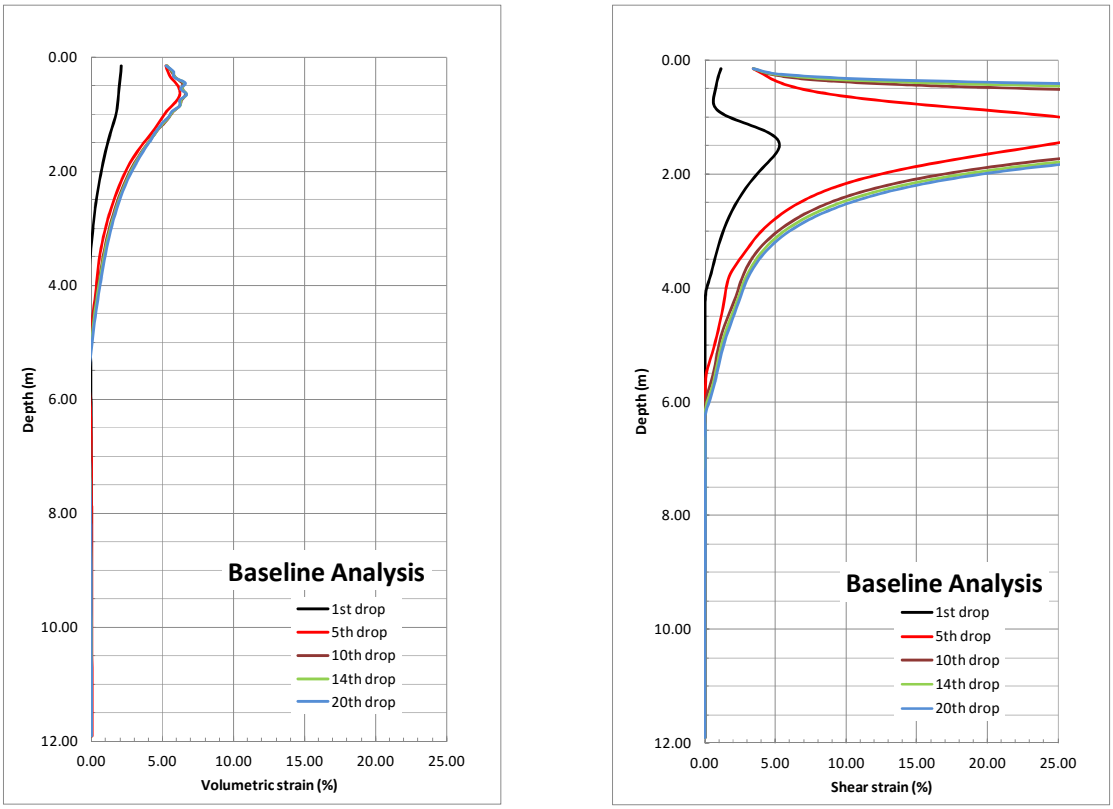

Figure 7.13: Evolution of volumetric and shear strains with depth and number of drops at the center of the pounder

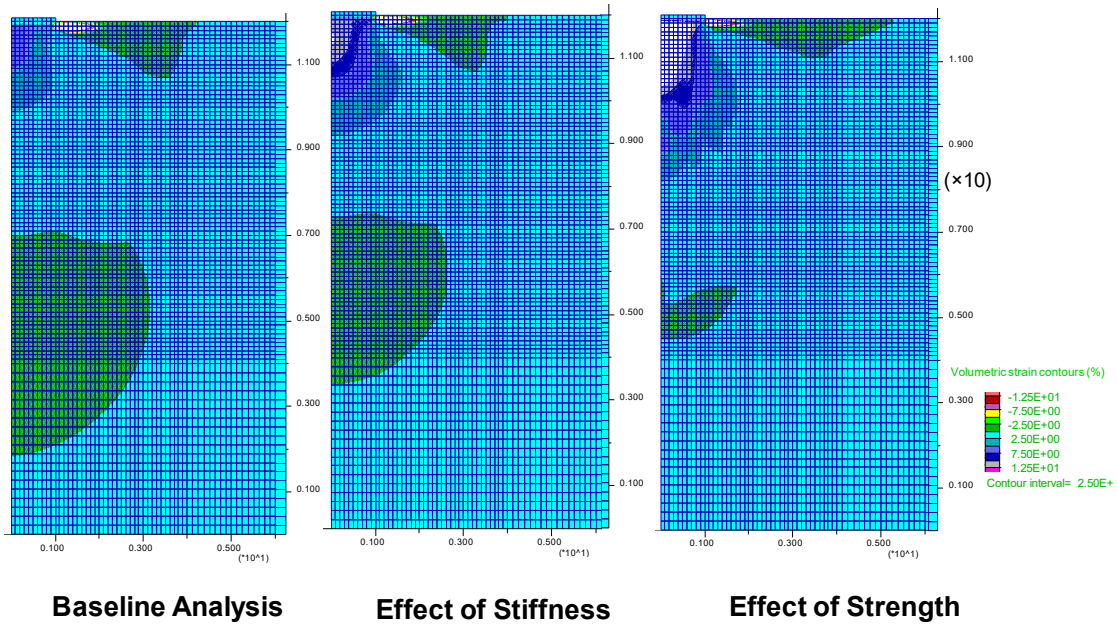

Figure 7.14: Effect of soils stiffness and strength on volumetric strains at 14th drop

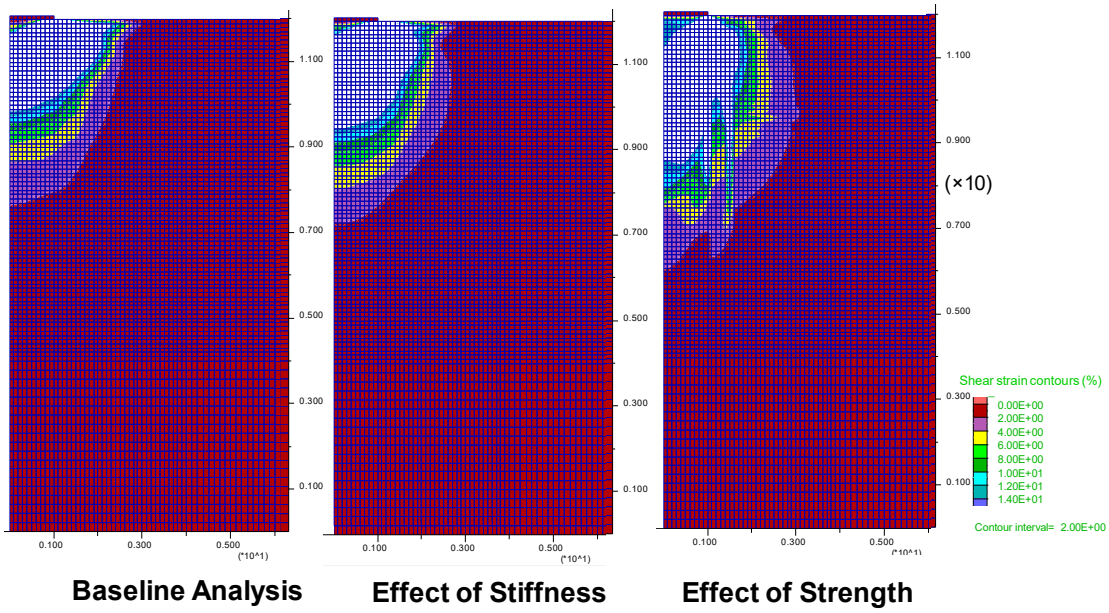

Figure 7.15: Effect of soil stiffness and strength on shear strains at the 14th drop

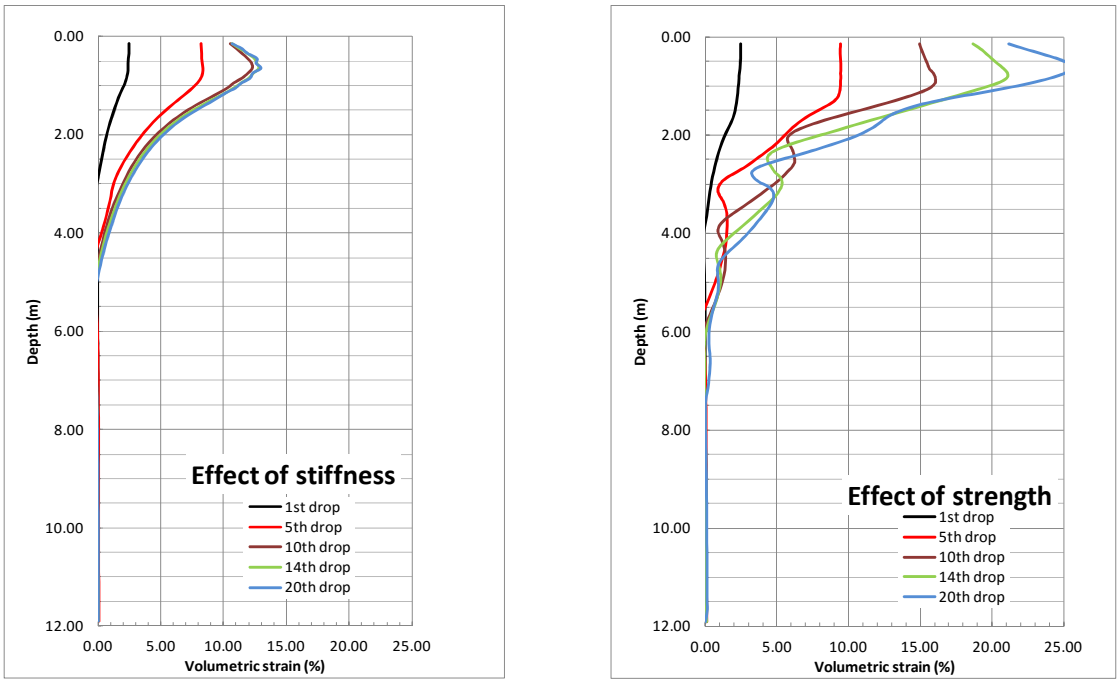

Figure 7.16: Effect of soil properties on the evolution of volumetric strains with depth and number of drops

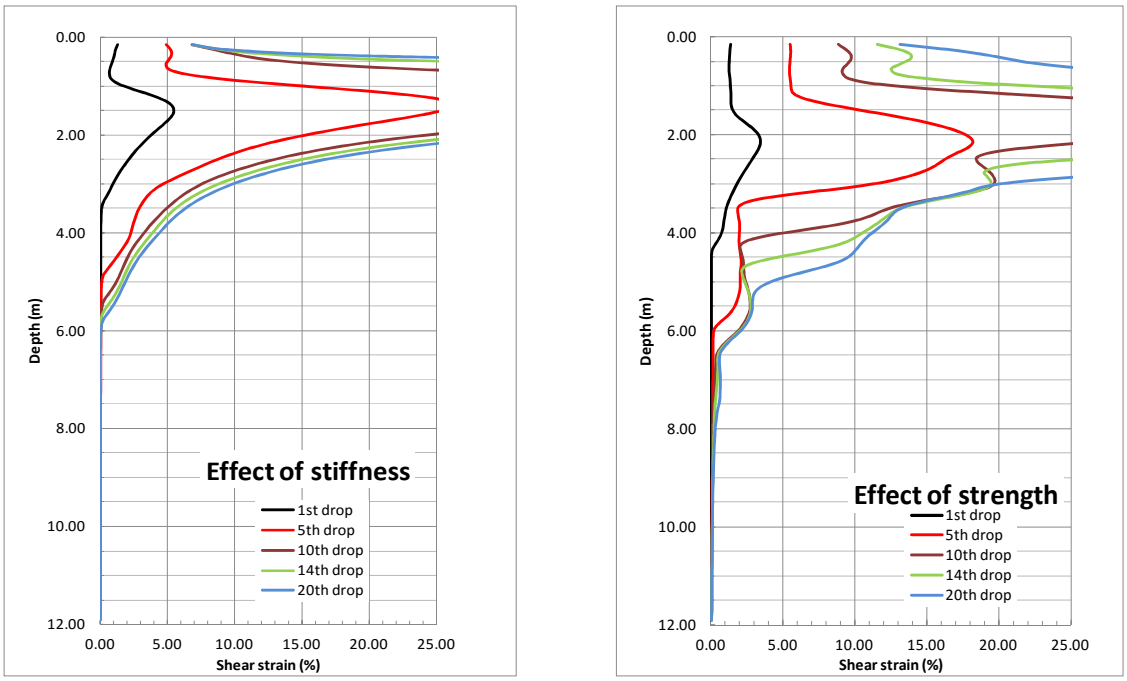

Figure 7.17: Effect of shear strains with depth and number of drops

CHAPTER 8: SUMMARY, CONCLUSIONS AND RECOMMENDATIONS

8.1 INTRODUCTION

Dynamic compaction (DC) is one of the most widely used ground improvement technologies to densify soils in-situ and improve their properties in depth. The technique is particularly effective for moist or saturated cohesionless soils that are largely free draining as well as finer soils above the water table.

Furthermore, in the last years several motorways are under construction in Romania. The author was involved as chief engineer with three motorway projects where DC was used for improving over 500,000 m^2 of soil, mostly loess. In the context of one of these projects he was directly responsible for designing and executing DC on a 40,000 m^2 experimental site and interpreting the results.

This report presents the results from the experimental site where DC was used to improve the bearing capacity of the soil, reduce differential settlements, and reduce the possibility of soil collapse. The densification scheme and site characterization results before and after improvement are presented and compared to the results of a finite difference numerical model.

8.2 RESEARCH OBJECTIVE AND PROJECT SCOPE

Based on the effectiveness of DC, its versatility and low cost this study was initiated based on the interest of using high energy DC for treating collapsible loess. This report presents site characterization and ground improvement performance results obtained from a 40,000m^2 experimental site in Constanta, Romania. The scope of the improvement was to treat the ground to depths ranging from 6 to 8 meters in order to reduce settlements and mitigate collapse potential.

To achieve this objective, it was necessary to establish improvement criteria (in situ, laboratory), to execute special compaction tests and determine the DC parameters (energy, number of drops, number of phases, etc.) based on actual results from the experimental site. In situ and laboratory results from the experimental site are compared to the results of a finite difference numerical model, developed to simulate the dynamic compaction. Other research topics involved application of this technique to waterfront projects and induced vibrations.

8.3 EXPERIMENTAL SITE

The experimental site is approx. 40,000 m^2 and located at Valul lui Traian (Constanta) in the vicinity of the railway line Bucharest – Constanta. On this site was performed high energy Dynamic Compaction (DC) to treat collapsible loess, as well as the quality tests presented herein.

The geometrical features of the experimental site are the following:

- length = 490 m
- maximum width = 83 m
- minimum width = 80 m
- total area = 39,997 m^2
- area compacted = 30,176 m²

Prior geotechnical investigations revealed the existence of a 12 m thick loess deposit below which is a layer of red clay with limestone concretions. It was determined that the first 6 meters of loess were sensitive to water. Under depths of about 28 m to 40 m is bedrock which consists of degraded limestone in clay mass. Groundwater level has been measured to depths below 12 meters.

8.4 RESULTS

In terms of underwater projects and according to Chapter 4 we have:

- Special considerations are necessary for laying out the drop points, which typically have to overlap, for the material used for the levelling phase, and the shape of the pounder.
- The water depth should be of minimum 4 m in order to obtain an effective compaction for a layer of maximum 2 m thickness.
- For smaller water depths, will be analyzed the possibility of applying DC in "dry conditions", by filling the area with cohessionless soil that later will be dredged.

The main results from obtaining measurements from a seismograph during construction and comparing it to literature (Chapter 5) are:

- Vibration frequency is influenced by the number of free falls - this is more evident at smaller distances;
- Soil particle velocity increases slower to a total number of four drops; after that it increases faster;
- The use of an isolation trench reduced with approximately 20% the velocity of soil particles;
- Soil particle velocity decreases with distance.

Chapter 6 provides the results obtained from the experimental site. From compaction tests was determined the response of collapsible loess to 1st and 2nd phase compaction effort:

	U.M.	12 blows	14 blows
Pounder penetration	(m)	2.19	2.34
Crater average volume	(m^3)	12.44	13.76
Enforced settlement	(cm)	25.4	28.1
Resulting volume reduction	(%)	4.23	4,68

and

	U.M.	12 blows	14 blows
Pounder penetration (m)	(m)	1.79	1.88
Crater volume	(m^3)	9.81	11.26
Enforced settlement	(cm)	20.00	23.00
Volume reduction	(%)	3.34	3.83

For certification of improvement was established the following requirements:

- Decreasing the additional settlement index $i_{m300} < 2\%$;
- Increasing the dry density $\rho_d > 1.6 g/cm^3$;
- Reduction of the porosity $n < 40\%$;
- Increasing the average oedometer modulus $M_{200\text{-}300}$ at natural moisture and saturation;
- Increasing the average tip resistance $q_c > 2.5MPa$;

After execution of DC it has been demonstrated that collapse risk was mitigated since:

- The additional settlement is eliminated (average $i_{m300} = 0.43\%$);
- Reduction of average n to 35%;
- Increasing of the dry density average $\rho_d = 1.75$ g/cm^3;
- The odometer modulus increased for both natural moisture and saturation conditions;
- The average cone resistance increased $q_c = 2.5 – 3.5$ MPa (> 2.5 MPa);

Chapter 7 presents and discusses the results of a numerical methodology, developed for the simulation of the method at the 40,000 m^2 experimental site, using the available site characterization data. The main assumptions of the numerical methodology were evaluated by performing sensitivity analyses. While the limitations of this model have been explained in Chapter 7, major results indicate that:

- The simplified model can, in a qualitative sense, predict the impact of the energy input on the local soils. The shape of the volumetric and shear strain contours is generally reasonable. The model indicates significant changes in the soil (in terms of volume and shear) below the tamper for a prescribed energy input.

- Values for the various parameters of the used model were selected based on a review of the site characterization data. The effect of the soil stiffness and strength on the numerical predictions was examined through sensitivity analysis. The results were evaluated mainly in terms of the developing strains and influence depth. Note also that the results of the analyses are sensitive to the values of the model parameters; hence particular attention is required in their selection.

- The depth of improvement is found to be in the order of 4-6 m for the baseline case, which is comparable to a depth of improvement of 7 m using the empirical Menard formula and somewhat lower than the values measured in the field (which varied from 6 m to 9 m). The reason for this bias is associated with two main factors: (a) the limitations of the model and potential variations in the material properties.

8.5 PERSONAL CONTRIBUTIONS

The main personal contributions included in the present thesis are:

1. State-of-the-art literature review and synthesis in the field of dynamic compaction and treatment of loess deposits using numerical modelling.
2. Analyzing in detail the concept of collapsible loess which leads to a better classification among difficult soils.
3. Experimental research by designing, executing and interpreting results from experimental pilot tests.
4. Design and execution of the experimental pilot test with the area of 40,000 m^2.
5. Analysis of the experimental site results.
6. Practical recommendations for the use of DC for marine applications; recommendations as a function of water depth for the necessary energy and shape and weight of the pounder.
7. Recommendations for applying DC for the treatment of loess: porosity, density, number of craters, number of blows, number of execution phases, and determination of the empirical coefficient a, which in turn is used to determine the depth of improvement, as well as, vibration related considerations.

8. Confirmation of experimental results with the use of numerical analysis.
9. Recommendations for future research.

8.6 RECOMMENDATIONS

Based on the limitations of the numerical modelling identified in Chapter 7, following are some specific recommendations for future work. Two approaches are recommended in order to establish a methodology for assessing improvement for use as a practical tool in engineering practice:

- The first approach involves the calibration of the current model against well documented case history to assess the systematic bias associated with the simple model used in order to generate recommendations with regards to the various aspects associated with the improvement. For example, correction factors can be applied to "correct" the model prediction against field performance.

- The second approach involves the development of a more comprehensive model that will more realistically capture the behavior of the soil. Such models, may be based on critical state plasticity, and will involve an updating methodology so that the stiffness and strength characteristics are revised as the void ratio of the soil changes due to volumetric compression or shearing. Incorporation of such model is likely to lead to improved relationships between the number of drops and the crater settlement (that will no longer be linear), the depth of improvement and possibly more reliable volume calculations. A disadvantage of such approach is that it will no longer be a simplified approach. The required computational time will increase significantly, and may render such analyses cumbersome. To address this issue, additional optimization work would be required.

In terms of general recommendations, to advance engineering and construction practice, this technique should be standardized by the European Committee for Standardization, while ground improvement contractors and universities should work together to advance the modelling of dynamic compaction by numerical modelling.

SELECTIVE REFERENCES

ASTM = American Society for Testing and Materials

C = Normativ

FHWA = Federal Highway Administration

NP = Reglementare tehnica

STAS = Standard de stat

SREN = Standard European

ASTM D 5333-92. Standard Test Method for Measurement of Collapse Potential of Soil.

ASTM D 2435-96. Standard Test Method for One-Dimensional Consolidation Properties of Soil.

C 29:1985. Normativ privind imbunatatirea terenurilor de fundare slabe prin procedee mecanice.

Ciortan, R., Tsitsas, G., 2012. "Vibratii ale terenului induse de compactarea dinamica intensiva," A XII-a Conferinta Nationala de Geotehnica si Fundatii – Iasi, pp 1-8.

FHWA, 1995. Dynamic Compaction, FHWA-SA-95- 037.

Ghassemi A., Pak A., Shahir H., 2009. "A numerical tool for design of dynamic compaction treatment in dry and moist sands," Iranian Journal of Science & Technology, Vol. 33, NoB4, pp 313 – 326.

Hayward Baker. "Project Summary: Dynamic Deep Compaction & Vibro-Compaction".

Holtz, R., Kovacs, W., 1981. An introduction to Geotechnical Engineering. Inc., Prentice-Hall, New Jersey, pp 299-309.

Itasca, 2005. "FLAC: Fast Lagrangian Analysis of Continua," Online Manual.

Lukas, R. G., 1995. Geotechnical Engineering Circular No.1: Dynamic Compaction, Ground Engineering Consultants Inc., USA.

Lutenegger, A., 1986. "Dynamic Compaction in Friable Loess," Journal of Geotechnical Engineering, Vol. 112, pp 663-666.

Manea, S., Ciortan, R., Tsitsas, G., Dumitru, M., 2012. "Verification of improvement for collapsible soils treated with High Energy Dynamic Compaction," Proceedings of the 12th National Conference in Geotechnical and Foundation engineering, vol. 1, pp. 77-85 in Iasi, Romania.

Ménard,, L. (1974). "La consolidation dynamique des sols de fondation." Revue des Sols et Foundations No. 320.

Ménard, L., Broise, Y., 1975. “Theoretical and Practical Aspects of Dynamic Consolidation,” Goetechniqué, Vol.25, 1, pp 3-19.

Mitchell, J. K., 1981. “Soil Improvement – State – of – the – Art – Report,” Proceeding 10th International Conference on Soil Mechanics & Foundation Engineering, Stockholm, Sweden, 4, pp 509-532.

Mitchell, J. K; Gardner, W. S., 1975. "In Situ Measurement of Volume Change Characteristics," SOA paper to Session IV, Proc. ASCE Conf. on In Situ Measurement of Soil Properties, Raleigh, N.C.; Vol. II, pp 279-346.

NE 008-1997. Normativ privind imbunatatirea terenurilor de fundare slabe prin procedee mecanice.

NP 125:2010. Normativ privind fundarea constructiilor pe pamanturi sensibile la umezire.

Romanian Design Normative NP 125, 2010 regarding Foundation on water sensitive soil.

Romanian Standard STAS 3300-2, 1985 regarding the Foundation soil – Calculation of foundation soil for direct foundations.

Rouaiguia A., Al-Zahrani R., 2002. “Simulation of soil dynamic compaction,” The 6th Saudi Engineering Conference, KFUPM, Dhahran, Vol.3, pp 223 – 232.

Sedovic, W., 1984. „Assesing the Effect of Vibration on Historic Building,” Bulletin of the Association for Preservation Technology, 16, pp 53-60.

STAS 8942/1-1989. Determinarea compresibilitatii pamanturilor prin incercarea in edometru

SREN 1997 – 2 – 2007. Eurocod 7: Proiectarea geotehnica – Partea 2: Investigarea si incercarea terenului.

Svinkin, M. R., Shaw, A. G., and Williams, D., 2000. „Vibrations Environmental Effect of Construction Operations,” DFI 25th Annual Meeting and 8th International Conference and Exhibition, A Global Perpective on Urban Deep Foundations, Deep Foundation Institute, Englewood Cliffs, N.J., pp 483-491.

Terashi, M., Juran, I., 2000. “Ground Improvement – State of the Art,” Proceedings International Conference on Geological & Geotechnical Engineering, GeoEng2000, 1, pp 461-519, Melbourne.

Tsitsas, G., Dimitriadi, V., Zekkos, D., Dumitru, M., Ciortan, R., Manea, S., 2015. “Dynamic Compaction of Collapsible Soil – Case Study from a Motorway Project in Romania,” Proceedings of the XVI European Conference on Soil Mechanics and Geotechnical Engineering, Edinburg, Vol. 3, pp 1487-1492.